RESPONSE OF BEAMS RESTING ON LINEAR AND NON-LINEAR ELASTIC FOUNDATIONS AND SUBJECTED TO HARMONIC HIGH-SPEED MOVING LOADING

Askar Ibrayev, BEng in Civil Engineering

Submitted in fulfillment of the requirements for the degree of Masters of Science in Civil Engineering

School of Engineering

Department of Civil and Environmental Engineering

Nazarbayev University

53 Kabanbay Batyr Avenue,

Astana, Kazakhstan, 010000

Supervisor: Jong Kim

Co-Supervisor: Desmond Adair

January 2018

DECLARATION

I hereby, declare that this manuscript, entitled “Response of Beams Resting on Linear and Non-Linear Elastic Foundations and Subjected to Harmonic High-Speed Moving Loading”, is the result of my own work except for quotations and citations which have been duly acknowledged.

I also declare that, to the best of my knowledge and belief, it has not been previously or concurrently submitted, in whole or in part, for any other degree or diploma at Nazarbayev University or any other national or international institution.

Name: Askar Ibrayev

Date: January 28, 2018

Abstract

Analytical solution technique that provides fast, efficient and accurate results is developed for the fourth-order nonlinear differential equations describing the transverse vibrations of a beam on an elastic foundation. The method of solution developed is based on a recent novel method of calculation, the Adomian Modified Decomposition Method (AMDM). AMDM has advantages of solving without discretization, linearization, perturbation, or a priori assumptions, all of which has the potential to change the physics of the problem. The accuracy and the convergence speed of the method are validated against exact solutions. The beam is analyzed using two existing beam theories, namely, Euler-Bernoulli and Timoshenko beam theories. For the foundation widely used one-parameter Winkler and two-parameter Pasternak foundations are used. Numerical calculations of vibration frequencies and mode shape functions are performed. Effect of a foundation parameters and loadings on beam vibrations are analyzed and discussed.

Acknowledgements

I would like to express my sincere gratitude to my supervisors Prof. Desmond Adair and Prof. Jong Kim for the continuous support on my thesis, for their motivation and immense knowledge. I am appreciative for all the hours of discussion they have offered me. It has been their supervision and direction throughout the duration of my studies which has allowed me to successfully complete this Master's program.

Table of contents

List of Abbreviations & Symbols

a	coefficient of rotary inertia
A	cross-section area
A_n	the Adomain polynomials
ADM	Adomian Decomposition Method
AMDM	Adomian Modified Decompositon Method
b	coefficient of shear deformation
BVP	Boundary Value Problem
C_m	AMDM coefficient
D	number of separate impulses
DQEM	Differential Quadrature Element Method
DTM	Differential Transform Method
e	coefficient of elastic layer stiffness
E	modulus of elasticity
G	modulus of rigidity
G^{-1}	four fold inverse operator
$h(t)$	harmonic function of time t
$H(:)$	Heaviside function
HPM	Homotophy Perturbation Method
I	cross-sectional moment of inertia
$k_{L0}, k_{L1}, k_{R0}, k_{R1}$	flexible end boundary coefficients
k_w	coefficient of foundation stiffness
k_p	coefficient of foundation shear
K_0	non-dimensional coefficient of foundation stiffness
K_1	non-dimensional coefficient of foundation shear
l	length of a beam
$M(x,t)$	bending moment
Nu	nonlinear term
ODE	Ordinary Differential Equation
p	pressure
P_0	load
$\bar{P}$	non-dimensional load
q	loading
Q	non-dimensional loading
r	span of load

s	coefficient of shear layer stiffness
t	time
T	kinetic energy
u	axial displacement
U	strain energy
v	velocity
$V(x,t)$	shear
VIM	Variational Iteration method
$w(x,t)$	vertical deflection of a beam
W	work done
$W(x)$	normalized beam vertical deflection
x	distance
X	non-dimensional distance
δ	infinitesimal interval
ε	error, pre-set sufficiently small value
ζ_m	coefficient of non-linear term
θ	rotation
$\Theta(x)$	normalized beam slope
κ	shear coefficient
κ_{L0}	dimensionless flexible end boundary coefficient
λ	eigenvalue of dimensionless natural frequency
ρ	density
$\phi(x)$	beam vertical deflection
$\bar{\phi}_i^{[n]}(X)$	normalized mode shape function
$\Phi(X)$	polynomial depending on the boundary conditions
$\psi(\mathrm{x},\mathrm{t})$	beam deflection
ω	circular frequency
Ω	dimensionless natural frequency

List of Tables

List of Figures

Chapter 1 – Introduction

1.1 General

High-speed railways are gaining broad interest around the world due to their transportation speed and efficiency. However, one of the drawbacks of high-speed trains is track vibration and induced noise they produce. Excessive track vibration can increase repair and down time of the track, necessitate the reduction of train maximum allowable speed, and reduce train service lifetime and also reduce riding comfort of passengers. In addition nearby infrastructure and residents are disturbed by ground vibrations produced by passing trains. Therefore the vibration response of the railway track to moving loads is of interest in the area of high-speed railway transportation. Foundation type and soil medium supporting the rails has also considerable effect on actual behavior of railway track.

In order to develop a theoretical model, simple, though realistic, geometries of rails and subsoil are considered. It is assumed that the railway track acts as a supported finite beam resting on an elastic foundation, which is modeled using springs. This model makes it possible to develop mathematical formulations based on the existing beam and foundation theories.

The aim of this work is the development of fast, efficient and accurate solution techniques for the fourth-order nonlinear differential equations which

describe accurately the transverse vibrations on an elastic foundation. The equations will describe the beam vibration responses depending on their type of beam model used, supporting foundation, and, the boundary and loading conditions.

1.2 Methodology and techniques

This works is built on existing theoretical frameworks that analysis classical problems related to beams resting on elastic foundations but with the provision of a new analytical solution method. The beam will be analyzed using two existing beam theories, namely, Euler-Bernoulli and Timoshenko beam theories. For the foundation widely used one-parameter Winkler and two-parameter Pasternak foundations will be used. To investigate the interaction and effect of parameters on the beams behavior different combinations of beam and foundation types are considered. This research includes the development of the solution method. First of all, Euler-Bernoulli beam resting on a Winkler foundation and Timoshenko beam resting on a Pasternak foundation are considered with no loading imposed. Later, non-moving and moving loading terms are introduced, with the speed and frequency of the moving loads are kept constant.

The method of solution developed is based on a recent novel method of calculation, namely, the Adomian Modified Decomposition Method (AMDM) in which Adomain polynomials can be used to treat the non-linear terms. This

method has been used in other applications to provide fast and accurate results [1,2]. In addition, compared to other existing methods the AMDM has advantages of solving without discretization, linearization, perturbation, or a priori assumptions, all of which has the potential to change the physics of the problem [3].

Although the AMDM has been used for solving problems related to beam responses, it has not been applied for finite beams resting on foundations subjected to harmonic loading. Moreover, beams on foundation will be investigated under axial loading. These are the originality of the present work which will be analyzed in following sections.

1.3 Literature review

1.3.1 Beams and Foundations

Modeling the interaction between the beam and the foundation is important for the analysis of the beam vibration. The supporting foundation is mostly modeled by simple spring elements, since it is mainly the beam that is being investigated. In order to make the model more realistic the shear parameter is introduced. Spring stiffness and shear layer describes the behavior of the elastic foundation. There have been several models developed for the foundation simulation that vary according to the use of parameters.

One of the models of subsoil mostly used due to its simplicity is Winkler foundation model. The concept is based on representing the soil as closely spaced, infinite but mutually independent elastic springs [4]. Because of the independency of each spring the foundation deformation occurs at loaded region only. The physical representation of the model is illustrated in Figure 1.1

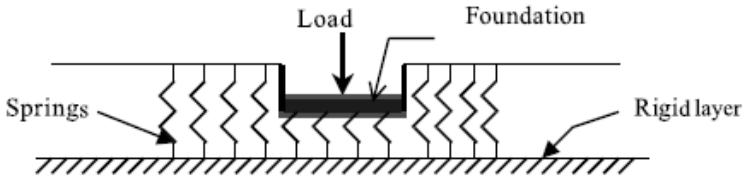

Figure 1.1 Winkler foundation model

Idealization and simplification of the foundation by Winkler model made it possible to use it widely for number of studies [4] on soil-structure behaviors. However, there are several disadvantages of Winkler model. The model does not allow the gradual distribution of the load over an influence area in term of the depth of load effect. This is due to the behavior of the independent springs. As a result, the load is concentrated only on the area of the subgrade where it is applied, which implies that the soil has no cohesion of its particles.

To overcome the limitation of relatively simple Winkler model, Pasternak model was introduced. The model has the assumption of shear interaction between the springs that create the shear effect of the foundation. It is made possible by implementing the layer that connects the springs and undergoes vertical shear deflection only [5]. The model is represented in Figure 1.2.

The relationship of a pressure-deflection can be represented as

$$p = kw - G\nabla^2 w \tag{1.4}$$

where p represents the pressure, k represent the coefficient of foundation stiffness, and w is the transverse deflection, G is the shear modules.

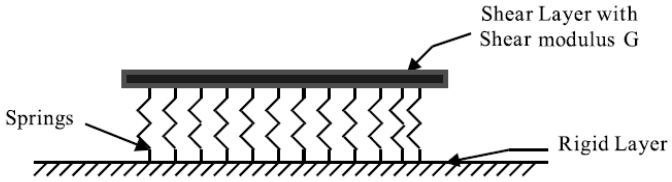

Figure 1.2 Pasternak foundation model

Thus by introduction of the shear layer the continuity within the soil medium is achieved.

There are several other specific however not widely used modifications of the initial spring model. Filonenko-Borodich model [6] replaces the shear layer of Pasternak model by tension layer as its physical equivalency. Kerr foundation presents the shear layer which is located in the middle of springs and implies that the stiffness of springs above and below the layers is different [7]. Another foundation model, which has different approach of formation, is Vlasov model. It has been developed based on the variational principle using elastic continuum approach to determine the parameters [8].

1.1.1 General methods for beam vibrations analysis

Recently, investigating the dynamic response of beams on elastic subsoil under moving loads is gaining great interest in railway engineering. Lee [9] analyzed the dynamic response of a Timoshenko beam under a moving load using a Winkler foundation. Thambiratnam and Zhuge [10] investigated the dynamic response of beams on an elastic support under moving mass by the use of finite element method. Both of them investigated how the stiffness of the foundation affects, the speed of travel and length of a beam on the factor of dynamic magnification. The vibration of an infinite Euler-Bernoulli beam on a Winkler foundation undergoing an axial force subjected to a harmonic and static moving mass was investigated by Kim [11] along with the stability of a beam. Other parameters such as the influence of a speed and frequency of load, critical velocity of the moving load, damping, frequency of vibration, and effect of the axial force are studied as well. The vibration response of an infinite Timoshenko beam resting on a Pasternak viscoelastic foundation and leaded by distributed harmonic moving mass was investigated by Kargarnovin and Younesian [5]. They also studied the dynamics of a Timoshenko and Euler-Bernoulli beams of an infinite length resting on nonlinear viscoelastic foundations and subjected to harmonic moving loads [12].

Euler-Bernoulli beam of a finite length on a nonlinear elastic foundation subjected to a concentrated moving loading was studies by Alkim *et al* [13].

There are several different methods of solution that can be utilized to solve vibration responses based on the level of difficulty of an equation and beam and foundation theories. They can be listed as follows:

- Differential Transform Method (DTM)
- Homotopy Perturbation Method (HPM)
- Variational iteration method (VIM)
- Differential quadrature element method (DQEM)
- Adomian Decomposition method (ADM)

Balkaya *et al* [14] applied DTM for the analysis of a vibration response of a Euler-Bernoulli beam resting on an elastic foundation whereas Ozturk and Coskun [15] applied HPM for the analysis of the same beam-foundation formulation. Chen [16] investigated the vibration response of a beam with the use of DQEM. He explained a method that consists of a mix of free vibration and bending of a beam on a Pasternak foundation model. HPM method was used in literature [17] to determine the frequency of the vibration of an Euler-Bernoulli beam resting on an elastic foundation, where the width of a foundation changes both linearly and exponentially.

1.1.2 Adomian Decomposition Method

The ADM is the method that provides analytical solution for the ordinary and partial differential equations. It was initially developed by George Adomian in 1980s [18]. This method is effective in solving differential equations that

involve non-linear functions. The principle of the ADM is based on its ability to create analytical expression that provide continuity solution domain [19]. In literature [20,21] it has been verified that it solves linear and non-linear equations accurately both being efficient and simple. ADM considers the sum of series that converge quickly [22]. The convergence accuracy of ADM has been studied in several literatures [23,24]. Wazwaz and Khuri investigated the use of ADM to solve Fredholm integral equations that describe particular acoustic equations [25]. Wazwaz also studied the ADM by comparing it to the Taylor series method and showed that the ADM results converges faster providing more accurate results [26]. One of the important aspects of the ADM is the use of special polynomials called ‘Adomian polynomials’ which decompose the non-linear part without linearizing it [19].

Chapter 2 – Theory development

2.1 Beam and foundation theory

2.1.1 Euler-Bernoulli beam resting on a Winkler foundation

The theoretical model consisting of a uniform Euler-Bernoulli beam on a Winkler foundation will be utilized to develop the mathematical formulation and solution method. As illustrated on Figure 1 the beam has a uniform rectangular cross-section area, A, a length, l, a cross-sectional moment of inertia, I, and, an isotropic beam with a modulus of elasticity, E, and density, ρ.

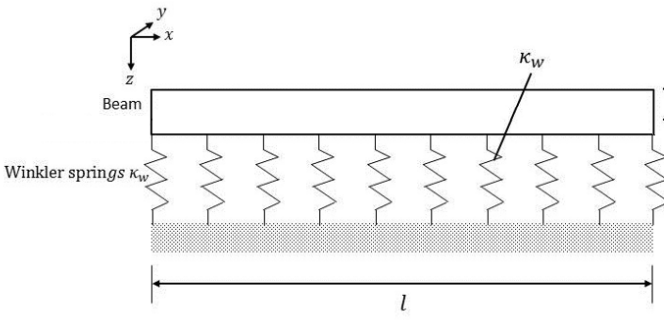

Figure 2.1 Beam resting on a Winkler foundation

The model for the foundation is the relatively simple Winkler foundation model whose stiffness is constant and does not change along the beam.

According to the Euler-Bernoulli beam model, the strain energy induced by displacement amplitude is given by

$$U = \frac{1}{2}\int_0^l EI\left(\frac{\partial^2 w(x,t)}{\partial x^2}\right)^2 \mathrm{d}x + \frac{1}{2}\int_0^l EA\left(\frac{\partial u(x,t)}{\partial x} + \frac{1}{2}\left(\frac{\partial w(x,t)}{\partial x}\right)^2\right)^2 \mathrm{d}x + \frac{1}{2}\int_0^l k_w w(x,t)^2 \mathrm{d}x, \tag{2.1}$$

where u is the axial and w is the transverse displacement, and k_w is the coefficient of foundation stiffness. Here inclusion of nonlinear term is necessary for high amplitudes in Eq. (2.1). The kinetic energy is given by

$$T = \frac{1}{2}\int_0^l \rho A\left(\frac{\partial w(x,t)}{\partial t}\right)^2 \mathrm{d}x. \tag{2.2}$$

By using Hamilton's principle and the Lagrangian of a system

$$\delta \int_{t_1}^{t_2} (T - U)\mathrm{d}t = 0. \tag{2.3}$$

and by substituting Eq. (2.1) and Eq. (2.2) into Eq. (2.3) the following governing equation is obtained

$$EI\frac{\partial^4 w(x,t)}{\partial x^4} + \rho A\frac{\partial^2 w(x,t)}{\partial t^2} + k_w w(x,t) - \frac{EA}{2l}\frac{\partial^2 w(x,t)}{\partial x^2}\int_0^l \left(\frac{\partial w(x,t)}{\partial x}\right)^2 \mathrm{d}x = 0. \tag{2.4}$$

By using the modal analysis for harmonic free vibration, $w(x,t)$ is separated in space and time as

$$w(x,t) = \phi(x)h(t) \tag{2.5}$$

where $\phi(x)$ is the modal deflection and $h(t)$ is a harmonic function of time t. Denoting the circular frequency of $h(t)$ by ω, then $\partial^2 w(x,t)/\partial t^2 = -\omega^2 \phi(x) h(t)$ and the eigenvalue problem of Eq. (2.4) becomes

$$EI\frac{\mathrm{d}^4\phi(x)}{\mathrm{d}x^4} - \frac{EA}{2l}\frac{\mathrm{d}^2\phi(x)}{\mathrm{d}x^2}\int_0^l \left(\frac{\mathrm{d}\phi(x)}{\mathrm{d}x}\right)^2 \mathrm{d}x + k_w\phi(x) - \rho A\omega^2\phi(x) = 0. \quad (2.6)$$

Eq. (2.6) is now made non-dimension by

$$X = \frac{x}{l}, \quad \phi(X) = \frac{\phi(x)}{l}, \quad K_0 = \frac{k_w l^4}{EI}, \quad \lambda = \frac{\rho A\omega^2 l^4}{EI},$$

and becomes

$$\frac{\mathrm{d}^4\phi(X)}{\mathrm{d}X^4} - \frac{1}{2}\frac{\mathrm{d}^2\phi(X)}{\mathrm{d}X^2}\int_0^1 \left(\frac{\mathrm{d}\phi(X)}{\mathrm{d}X}\right)^2 \mathrm{d}X + (K_0 - \lambda)\phi(X) = 0. \quad (2.7)$$

2.1.2 Timoshenko beam resting on Pasternak foundation

Despite the effectiveness of the Euler-Bernoulli beam theory on obtaining accurate results of vibration frequencies of slender beams, the Timoshenko beam theory predicts more accurate results on thick non-slender beams where shear or rotatory effects needs to be considered. The theory brought significant improvement in analysis of non-slender beams and is effective for higher frequency responses [27].

Kerr [7], states that the two-parameter Pasternak foundation is considered as one of the most used models and represents a more precise model of the foundation than the Winkler model.

Mathematical formulation

The Timoshenko beam theory with considerable shear and rotatory effects and the Pasternak foundation model, as illustrated on Figure 2.2 is used to obtain following derivation.

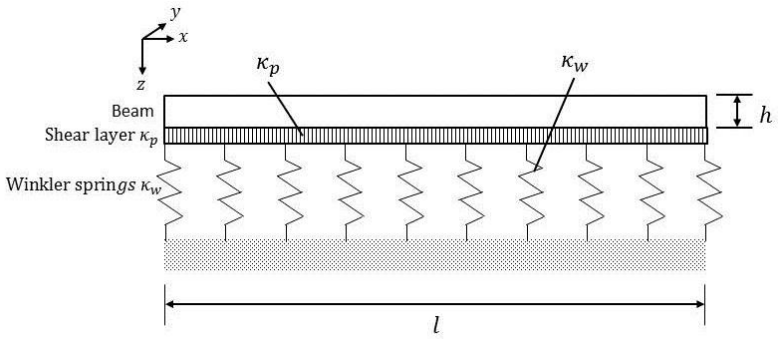

Figure 2.2 A beam on a Pasternak foundation

The Eq. (2.8) describes the potential energy of the beam-foundation system

$$U = \frac{1}{2}\int_0^l EI\left(\frac{\partial\theta(x,t)}{\partial x}\right)^2 \mathrm{d}x + \frac{1}{2}\int_0^l \kappa AG\left(\theta(x,t) - \frac{\partial w(x,y)}{\partial x}\right)^2 \mathrm{d}x + \frac{1}{2}\int_0^l k_w(w(x,t))^2 \mathrm{d}x + \frac{1}{2}\int_0^l k_p\left(\frac{\partial w(x,t)}{\partial x}\right)^2 \mathrm{d}x. \tag{2.8}$$

Here, l is the length of the beam, A the area of the cross-section, I the moment of inertia of the cross section, G the modulus of rigidity,E the modulus

of elasticity, κ the shear coefficient, k_w the coefficient of foundation stiffness, k_p the coefficient of foundation shear, $w(x,t)$ the vertical deflection and $\theta(x,t)$ is the beam slope of bending at location x and at time t.

The kinetic energy of the system is

$$T = \frac{1}{2}\int_0^l \rho A\left(\frac{\partial w(x,t)}{\partial t}\right)^2 \mathrm{d}x + \frac{1}{2}\int_0^l \rho I\left(\frac{\partial \theta(x,t)}{\partial t}\right)^2 \mathrm{d}x, \tag{2.9}$$

where ρ is density. The Hamilton's principle is used to obtain the equation of motion

$$\int_{t_1}^{t_2} \delta(T-U)\mathrm{d}t + \int_{t_1}^{t_2} \delta W \mathrm{d}t = 0. \tag{2.10}$$

where δW is the virtual work done, t_1 and t_2 are times and δ is infinitesimal interval showing the virtual change. By substituting Eqs. (2.8) and (2.9) into Eq. (2.10) two coupled equations are obtained for the vibration response

$$\begin{aligned}\rho A\frac{\partial^2 w(x,t)}{\partial t^2} + \kappa AG\left(\frac{\partial \theta(x,t)}{\partial x} - \frac{\partial^2 w(x,t)}{\partial x^2}\right) + k_w w(x,t) \\ - k_p\frac{\partial^2 w(x,t)}{\partial t^2} = 0,\end{aligned} \tag{2.11}$$

$$\begin{aligned}EI\frac{\partial^2 \theta(x,t)}{\partial x^2} - \rho I\frac{\partial^2 \theta(x,t)}{\partial t^2} \\ - \kappa AG\left(\theta(x,t) - \frac{\partial w(x,t)}{\partial x}\right) = 0.\end{aligned} \tag{2.12}$$

Eqs. (2.11) and (2.12) are now uncoupled to provide the general equation

$$EI\left(1+\frac{k_p}{\kappa AG}\right)\frac{\partial^4\psi(x,t)}{\partial x^4}+\left(\rho A+\frac{k_w\rho I}{\kappa AG}\right)\frac{\partial^2\psi(x,t)}{\partial t^2}$$

$$-\left(\frac{EIk_w}{\kappa AG}+k_p\right)\frac{\partial^2\psi(x,t)}{\partial x^2} \qquad (2.13)$$

$$-\left[\rho I\left(1+\frac{E}{\kappa G}\right)+\frac{k_p\rho I}{\kappa AG}\right]\frac{\partial^4\psi(x,t)}{\partial x^2\partial t^2}+\frac{\rho^2 I}{\kappa G}\frac{\partial^4\psi(x,t)}{\partial t^4}+k_w\psi(x,t)=0,$$

where, $\psi(\mathrm{x},\mathrm{t})$, is substituted as required by $w(x,t)$, for beam deflection and, by $\theta(x,t)$ for beam slope.

It is then assumed that the beam is excited harmonically with an angular frequency ω

$$w(x,t)=W(x)e^{i\omega t},\theta(x,t)=\Theta(x)e^{i\omega t},X=\frac{x}{l},\Omega^2=\frac{\rho Al^4}{EI}\omega^2,$$

where $i=\sqrt{-1}$, X is the non-dimensional length of the beam and $W(x)$ $\Theta(x)$ are the normalised functions of $w(x)$ and $\theta(x)$, respectively. Using these relationships Eq. (2.13) now becomes

$$\frac{\mathrm{d}^4\phi(X)}{\mathrm{d}X^4}+\lambda_1\frac{\mathrm{d}^2\phi(X)}{\mathrm{d}X^2}+\lambda_2\phi(X)=0, \qquad (2.14)$$

where $\phi(X)$, is substituted as required by $\Theta(X)$ for beam slope and, by $W(X)$, for beam deflection. Terms in Eq. (2.14) are expressed as

$$\lambda_1=\frac{\Omega^2(a^2+b^2)-b^2e^2+s^2(\Omega^2a^2b^2-1)}{1+b^2s^2},$$

$$\lambda_2=\frac{(\Omega^2-e^2)(\Omega^2a^2b^2-1)}{1+b^2s^2}.$$

where, a, b, e, s are the coefficients that describe rotary inertia, shear deformation, elastic layer stiffness and shear layer stiffness, respectively, as following

$$a^2 = \frac{I}{Al^2}, b^2 = \frac{EI}{\kappa GAl^2}, e^2 = \frac{k_w l^4}{EI}, s^2 = \frac{k_p l^2}{EI}$$

The ODE of Eq. (2.14) can be solved considering two conditions which give two solutions.

First condition is stated as follows

$\lambda_2 < 0$ which means$\{\ \Omega < \frac{1}{ab}$ and $\Omega > e\}$ or $\{\Omega > \frac{1}{ab}$ and $\Omega < e\}$

By using this condition the solution of ODE is expressed in terms of trigonometric and hyperbolic functions

$$\begin{aligned}\phi(X) = C'_1 \cosh(\alpha_1 X) + C'_2 \sinh(\alpha_1 X) \\ + C_3 \cos(\beta X) + C_4 \sin(\beta X)\end{aligned} \tag{2.15}$$

where

$$\alpha_1 = \frac{1}{\sqrt{2}} \sqrt{-\lambda_1 + \sqrt{\lambda_1^2 - 4\lambda_2}}$$

$$\beta = \frac{1}{\sqrt{2}} \sqrt{\lambda_1 + \sqrt{\lambda_1^2 - 4\lambda_2}}$$

Second condition is stated as follows

$$\lambda_2 > 0 \text{ which means} \{ \Omega > \frac{1}{ab} \text{ and } \Omega > e \} \text{ or } \{ \Omega < \frac{1}{ab} \text{ and } \Omega < e \}$$

As a result, the condition leads to the solution to be expressed in trigonometric functions only

$$\begin{aligned} \phi(X) = \bar{C}_1 \cos(\alpha_2 X) + \bar{C}_2 \sin(\alpha_2 X) \\ + \bar{C}_3 \cos(\beta X) + \bar{C}_4 \sin(\beta X) \end{aligned} \tag{2.16}$$

where

$$\alpha_2 = \frac{1}{\sqrt{2}} \sqrt{\lambda_1 - \sqrt{\lambda_1^2 - 4\lambda_2}}$$

$$\beta = \frac{1}{\sqrt{2}} \sqrt{\lambda_1 + \sqrt{\lambda_1^2 - 4\lambda_2}}$$

Thus the exact solution can be obtained for the governing equations describing Timoshenko beam behavior on the Pasternak foundation. As provided above two behaviors for the Timoshenko beam can be observed. Azevedo *et al*. [28] studied this phenomenon, which is called second spectrum phenomenon.

They explained the reason is due to the deviation of phase between the bending and shear deformation. First condition is the one that is usually studied for natural frequencies.

2.1.3 Boundary Conditions

Pinned-pinned, clamped-clamped and clamped free boundary conditions are described in this work. Boundary conditions for the pinned-pinned case in non-dimensional form at $X = 0$ and $X = 1$ are

$$\phi(X) = \frac{\mathrm{d}^2\phi(0)}{\mathrm{d}X^2} = 0. \tag{2.17}$$

Boundary conditions for the clamped-clamped case at $X = 0$ and $X = 1$ are

$$\phi(X) = \frac{\mathrm{d}\phi(X)}{\mathrm{d}X} = 0. \tag{2.18}$$

Boundary conditions for the clamped-free case at $X = 0$ and $X = 1$ are

$$\phi(0) = \frac{\mathrm{d}\phi(0)}{\mathrm{d}X} = 0, \qquad \phi(1) = \frac{\mathrm{d}^3\phi(1)}{\mathrm{d}X} \tag{2.19}$$

Boundary conditions are described in terms of rotational and translational flexible ends to make it convenient to use with the AMDM as shown on Figure 2.3.

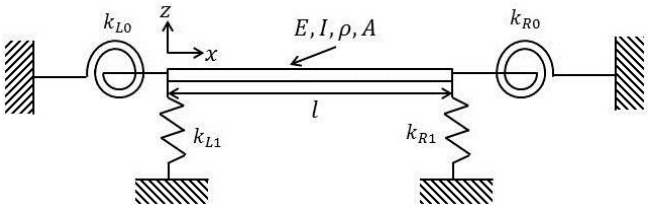

Fig. 2.3 Boundary condition described by rotational and translational flexible ends.

The boundary conditions are turned into dimensionless form as

$$\frac{\mathrm{d}^2\phi(0)}{\mathrm{d}X^2} - \kappa_{L0}\frac{\mathrm{d}\phi(0)}{\mathrm{d}X} = 0$$

$$\frac{\mathrm{d}^3\phi(0)}{\mathrm{d}X^3} + \kappa_{L1}\phi(0) = 0$$

$$\frac{\mathrm{d}^2\phi(1)}{\mathrm{d}X^2} + \kappa_{R0}\frac{\mathrm{d}\phi(1)}{\mathrm{d}X} = 0 \qquad (2.20)$$

$$\frac{\mathrm{d}^3\phi(1)}{\mathrm{d}X^3} - \kappa_{R1}\phi(1) = 0$$

where the coefficients are made non-dimensional using

$$\kappa_{L1} = \frac{k_{L1}l^3}{EI}, \quad \kappa_{R1} = \frac{k_{R1}l^3}{EI}, \quad \kappa_{L0} = \frac{k_{L0}l}{EI}, \quad \kappa_{R0} = \frac{k_{R0}l}{EI}$$

2.2 Adomian Decomposition Method

The Adomian Decomposition Method (ADM) decomposes an unknown function $u(x,t)$ of an equation into the summation of an infinite number of components defined by

$$u(x,t) = \sum_{n=0}^{\infty} u_n(x,t), \qquad (2.17)$$

where the components $u_n(x,t), n \geq 0$ are found recursively.

The ADM utilizes the method of finding the component $u_0, u_1, u_2, \ldots$ individually and the determination of these components are performed by recursive manner involving simple integration. Adomian decomposition consists of separating a given equation into linear and nonlinear parts, taking the inverse highest-order derivative operator, identifying the initial or boundary conditions

and the terms that consist of the independent variable as an initial approximation, decomposing the unknown function into a series for further determination of its components, decomposing the nonlinear functions into special polynomials so-called Adomian polynomials and finding the number of terms of the series solution recurrently using these polynomials. The solution is determined as an infinite series in which each term can be relatively easily found and follows the quick convergence that gives an accurate solution. The ADM is analytic, quantitative rather than qualitative, continuous and does not require perturbation, linearization and discretization.

To overview the ADM, consider the differential equation

$$Fu(t) = g(t), \tag{2.18}$$

where F is a general nonlinear ordinary or partial differential operator consisting of both linear and nonlinear terms. Linear components are decomposed into $L + R$ where L is invertible which is taken as the highest order derivative to overcome integrations with complicated Green's functions, and the remainder of the liner operator is defined by R. Eq. (2.18) is now written as

$$Lu = g - Ru - Nu, \tag{2.19}$$

where Nu describes any nonlinear components. L^{-1} is defined as the two-fold integration operator

$$L^{-1}\int_0^t\int_0^t(.)\mathrm{d}t\mathrm{d}t, \tag{2.20}$$

For the operator $L=\frac{\mathrm{d}^2}{\mathrm{d}t^2}$

$$L^{-1}Lu=u(x,t)-u(x,0)-tu_t(x,0), \tag{2.21}$$

and operating on both sides of Eq. (2.19) with L^{-1} gives

$$L^{-1}Lu=L^{-1}g-L^{-1}Ru-L^{-1}Nu. \tag{2.22}$$

Combining Eq. (2.21) and Eq. (2.22) yields

$$u(x,t)=u(x,0)+tu_t(x,0)+L^{-1}Ru-L^{-1}Nu. \tag{2.23}$$

The ADM represents the solution of $u(x,t)$ as a series of the form

$$u(x,t)=\sum_{n=0}^{\infty}u_n(x,t). \tag{2.24}$$

The nonlinear component Nu is decomposed as

$$Nu=\sum_{n=0}^{\infty}A_n. \tag{2.25}$$

Substituting Eq. (2.24) and (2.25) into Eq. (2.23)

$$\sum_{n=0}^{\infty}u_n(x,t)=u_0-L^{-1}R\sum_{n=0}^{\infty}u_n-L^{-1}\sum_{n=0}^{\infty}A_n, \tag{2.26}$$

where

$$u_0=f \tag{2.27}$$

and f is the terms that comes from integrating the source term g and from the initial or boundary conditions.

Consequently

$$\begin{aligned} u_1 &= -L^{-1}Ru_0 - L^{-1}A_0, \\ u_2 &= -L^{-1}Ru_1 - L^{-1}A_1, \\ &\vdots \\ u_{n+1} &= -L^{-1}Ru_n - L^{-1}A_n, \qquad n \geq 0, \end{aligned} \tag{2.28}$$

where A_n are the Adomain polynomials determined for each nonlinearity. The Adomain polynomials are derived from the formula

$$A_n = \frac{1}{n!}\frac{\mathrm{d}^n}{\mathrm{d}\lambda^n}[F(\sum_{n=0}^{\infty}\lambda^n u_n)]_{\lambda=0}, n = 0,1,2 \ldots \tag{2.29}$$

By using Eq. (2.29) the first five Adomian polynomials are

$$\begin{aligned} A_0 &= F(u_0), \\ A_1 &= u_1F'(u_0), \\ A_2 &= u_2F'(u_0) + \frac{1}{2!}u_1^2F''(u_0), \\ A_3 &= u_3F'(u_0) + u_1u_2F''(u_0) + \frac{1}{3!}u_1^3F'''(u_0), \\ A_4 &= u_4F'(u_0) + \left[\frac{1}{2!}u_2^2 + u_1u_3\right]F''(u_0) + \frac{1}{2!}u_1^2u_2F'''(u_0) \\ &\quad + \frac{1}{4!}u_1^4F''''(u_0), \\ &\vdots \end{aligned} \tag{2.30}$$

The practical solution for Eq. (2.25) is given as

$$\phi_n = \sum_{i=0}^{n-1} u_i, \tag{2.31}$$

where

$$u(x,t) = \lim_{n\to\infty} \phi_n(x,t) = \sum_{i=0}^{\infty} u_i(x,t). \tag{2.32}$$

It needs to be tested for the number of terms in order to obtain the convergence.

2.2.1 Adomian Modified Decomposition Method

There have been several modifications on the Adomian decomposition method made by different researchers in order to increase the convergence speed or to change the application of the original method. Wazwaz [1] proposed powerful modification of ADM, which showed rapid convergence compared to AMD. Adomian modified decomposition method has been proven to be easier to apply and computationally efficient in several examples [2].

The overview of basic theory of AMDM is stated as follows. Consider the equation

$$Fy(x) = g(x), \tag{2.33}$$

where F is a general non-linear ordinary differential operator involving both linear and non-linear components, and $g(x)$ is a given function. The linear terms

in Fy are decomposed into $Ly + Ry$ where L represents an invertible operator, which for AMDM is taken as the highest-order derivative and R represents the remainder of the linear operator. Eq. (2.33) can now be written as

$$Ly + Ry + Ny = g, \tag{2.34}$$

where Ny represents the non-linear terms of Fy and Eq. (2.34) describes an initial-value or boundary-value problem.

By solving Ly Eq. (2.34) becomes

$$y = \Phi + L^{-1}(g) - L^{-1}(Ry) - L^{-1}(Ny), \tag{2.35}$$

where Φ is the integration constant and $L\Phi = 0$ is satisfied. To use the AMDM y is decomposed into the infinite summation of a convergent series

$$y = \sum_{m=0}^{\infty} C_m x^m, \tag{2.36}$$

and the non-linear component is decomposed using Adomian polynomials, A_m,

$$Ny = \sum_{m=0}^{\infty} x^m A_m(C_0, C_1, \dots, C_m). \tag{2.37}$$

The function $g(x)$ is also decomposed as

$$g(x) = \sum_{m=0}^{\infty} g_m x^m. \tag{2.38}$$

On putting Eqs. (2.36)-(2.38) into Eq. (2.35) gives

$$y = \sum_{m=0}^{\infty} C_m x^m = \Phi + L^{-1}\left(\sum_{m=0}^{\infty} g_m x^m\right) - L^{-1}R\left(\sum_{m=0}^{\infty} C_m x^m\right) - L^{-1}\left(\sum_{m=0}^{\infty} x^m A_m\,(C_0, C_1, \dots, C_m)\right). \tag{2.39}$$

The coefficients C_m can be determined in a recurrence manner and the power series solutions of linear homogeneous differential equations in initial-value problems gives simple recurrence for the coefficients C_m. In fact the coefficients cannot be calculated exactly, and the truncated series $\sum_{m=0}^{n-1} C_m x^m$ will be used to approximate the solutions.

2.2.2 Adomian Polynomials for nonlinear term

To decompose the nonlinear components of differential equations Adomian polynomials are used. The accuracy of the solution depends on the number of terms for which the convergence is observed. In order to be able to create and calculate the series controlling the number of terms for the accurate results computer software is required.

The Eq. (2.29) describing Adomain polynomials is coded in MATLAB software. The code creates a series of any function describing the nonlinear term (Appendix A1). It is simple and compact, and can solve the function of any order and any type, including compound functions fast and accurately up to desired number of series. The result of u^4 and $\sin u$ is represented below as an example.

Adomian polynomials for u^4 up to 5 terms:

A(0)= u(0)^4

A(1)= 4*u(0)^3*u(1)

A(2)= 6*u(0)^2*u(1)^2 + 4*u(0)^3*u(2)

A(3)= 4*u(0)*u(1)^3 + 4*u(0)^3*u(3) + 12*u(0)^2*u(1)*u(2)

A(4)= 6*u(0)^2*u(2)^2 + 4*u(0)^3*u(4) + u(1)^4 + 12*u(0)*u(1)^2*u(2) +

12*u(0)^2*u(1)*u(3)

A(5)= 4*u(1)^3*u(2) + 4*u(0)^3*u(5) + 12*u(0)*u(1)*u(2)^2 +

12*u(0)*u(1)^2*u(3) + 12*u(0)^2*u(1)*u(4) + 12*u(0)^2*u(2)*u(3)

Adomian polynomials for $\sin u$ up to 5 terms:

A(0)= sin(u(0))

A(1)= u(1)*cos(u(0))

A(2)= u(2)*cos(u(0)) - (u(1)^2*sin(u(0)))/2

A(3)= u(3)*cos(u(0)) - (u(1)^3*cos(u(0)))/6 - u(1)*u(2)*sin(u(0))

A(4)= (u(1)^4*sin(u(0)))/24 - (u(2)^2*sin(u(0)))/2 + u(4)*cos(u(0)) -

u(1)*u(3)*sin(u(0)) - (u(1)^2*u(2)*cos(u(0)))/2

A(5)= (u(1)^5*cos(u(0)))/120 + u(5)*cos(u(0)) - u(1)*u(4)*sin(u(0)) -

u(2)*u(3)*sin(u(0)) - (u(1)*u(2)^2*cos(u(0)))/2 - (u(1)^2*u(3)*cos(u(0)))/2 +

(u(1)^3*u(2)*sin(u(0)))/6

2.3 Validation of Adomian Decomposition Method

Before using Adomian Decomposition Method to specific problems it is needed to show the accuracy by validating it against some known equations. The following equation will be considered for which there is exact solutions to compare with.

Consider a reasonably difficult general fourth-order integro-differential equation with two-point BVPs.

$$\frac{d^4y(x)}{dx^4} = f(x) + \gamma y(x) + \int_0^x [g(x)y(x) + h(x)F(y(x))]\mathrm{d}x \quad x \in (a,b) \tag{2.40}$$

where the boundary conditions are

$$y(a) = \alpha_0, \qquad y''(a) = \alpha_2$$

$$y(b) = \beta_0, \qquad y''(b) = \beta_2$$

F is a real non-linear continuous function, $\gamma, \alpha_0, \alpha_1, \beta_0, \beta_1$ are the real constants and f, g, h are given and can be approximated by Taylor series.

The fourth-order equation for the ADM can be written as

$$Gy = f(x) + \gamma y(x) + \int_0^x [g(x)y(x) + h(x)F(y(x))]\,\mathrm{d}x \tag{2.41}$$

where $G = d^4/dx^4$ which is used as the four-fold operator

$$G^{-1}(\cdot) = \int_0^x \int_0^x \int_0^x \int_0^x (\cdot)\mathrm{d}x\ \mathrm{d}x\ \mathrm{d}x\ \mathrm{d}x$$

Applying this operator to both sides gives

$$\begin{aligned} y = \sum_{j=0}^{3} \alpha_j \frac{x^j}{j!} + L^{-1}\big(f(x)\big) + G^{-1}\big(\gamma y(x)\big) \\ + G^{-1}\left(\int_0^x [g(x)y(x) + h(x)F(y(x))]\,\mathrm{d}x\right) \end{aligned} \tag{2.42}$$

The ADM takes the solution y and the non-linear function F as infinite series.

$$\begin{aligned} y &= \sum_{k=0}^{\infty} y_k \\ F &= \sum_{k=0}^{\infty} A_k \end{aligned} \tag{2.43}$$

The y_k are determined from the following recursive relation

$$\begin{aligned} y_0 &= \sum_{j=0}^{3} \alpha_j \frac{x^j}{j!} + G^{-1}(f(x)) \\ y_{k+1} &= G^{-1}(\gamma y_k) + G^{-1}\left(\int_0^x [g(x)y_k + h(x)A_k]\mathrm{d}x\right), \quad k \geq 0 \end{aligned} \tag{2.44}$$

where $\alpha_1 = y'(0)$ and $\alpha_3 = y'''(0)$ are to be determined and the Adomian polynomials A_k are given by

$$A_k = \frac{1}{k!}\left[\frac{\mathrm{d}^k}{\mathrm{d}\lambda^k} F\left(\sum_{j=0}^{\infty} \lambda^j y_j\right)\right]_{\lambda=0}, \quad k = 0,1,2, ... \tag{2.45}$$

Convergence aspects of the ADM have to be determined. For later numerical computation, let

$$\phi_n(x) = \sum_{k=0}^{n-1} y_k \tag{2.46}$$

denote the n-term approximation to $y(x)$.

It should be noted that α_1 and α_3 are not determined yet. Imposing the second line of boundary conditions above

$$\phi_n(b) = y_0(b) + y_1(b) + \cdots + y_{n-1}(b) = \beta_0$$

$$\phi_n''(b) = y_0''(b) + y_1''(b) + \cdots + y_{n-1}''(b) = \beta_2$$

from which the unknowns α_1 and α_3 can be determined.

2.3.1 Linear Boundary Value Problem

Consider the linear fourth-order integro-differential equation with $f(x) = x(1 + e^x) + 3e^x, \gamma = 1, g(x) = -1, h(x) = 0$, i.e.,

$$\frac{d^4y(x)}{dx^4} = x(1 + e^x) + 3e^x + y(x) - \int_0^x y(x)\mathrm{d}x, 0 < x < 1 \tag{2.47}$$

subject to

$$y(0) = 1, y''(0) = 2, y(1) = 1 + e, y''(1) = 3e$$

The exact solution is

$$y = 1 + xe^x \tag{2.48}$$

Adomian decomposition algorithm is written as follows

$$\begin{aligned} y_0 = &\quad 1 + Ax + x^2 + \frac{1}{3!}Bx^3 + G^{-1}(x + xe^x + 3e^x) \\ y_{k=1} = &\quad G^{-1}\big(y_k(x)\big) - G^{-1}\big(\textstyle\int_0^x y_k(x)\mathrm{d}x\big),\ \ k \geq 0 \end{aligned} \tag{2.49}$$

where $A = y'(0), B = y'''(0)$ are to be determined.

The integration of the last terms in Eq. (2.49) can be difficult. Therefore approximants like the truncated Taylor expansions will be considered for the exponential term in Eq. (2.49)

$$\begin{aligned} e^x &\sim 1 + x \\ e^x &\sim 1 + x + x^2/2! \\ e^x &\sim 1 + x + x^2/2! + x^3/3! \end{aligned} \tag{2.50}$$

It should be observed how the accuracy is affected by these truncations.

It can be shown that

$$\begin{aligned} \phi_{2,2}(x) = &\left(f_0 + \frac{1}{360}x^6\right) \\ &+ \left(f_1 - \frac{1}{1209600}x^{10} - \frac{1}{19958400}x^{11}\right) \end{aligned} \tag{2.51}$$

$$\phi_{2,3}(x) = \left(f_0 + \frac{1}{144}x^6 + \frac{1}{1680}x^7\right) + \left(f_1 - \frac{1}{19958400}x^{11} - \frac{1}{159667200}x^{12}\right)$$

$$\phi_{2,4}(x) = \left(f_0 + \frac{1}{144}x^6 + \frac{1}{840}x^7 + \frac{x^8}{10080}\right) + \left(f_1 + \frac{1}{39916800}x^{11} - \frac{1}{239500800}x^{12} - \frac{1}{1556755200}x^{13}\right)$$

The second subscript here refers to the number of terms used in the truncated Taylor expansions for e^x.

$$f_0 = 1 + Ax + x^2 + \frac{1}{6}Bx^3 + \frac{1}{8}x^4 + \frac{1}{24}x^5$$

$$f_1 = \frac{1}{24}x^4 + \frac{A-1}{120}x^5 + \frac{2-A}{720}x^6 + \frac{B-2}{5040}x^7 + \frac{3-B}{40320}x^8 + \frac{1}{181440}x^9 \qquad (2.52)$$

where A and B can be determined using the last two terms of the above boundary conditions. Imposing these boundary conditions on the Eq. (2.51) for ϕ, values for A and B is calculated and provided in the Table 2.1.

Table 2.1 Values of A and B for linear BVP

	$\phi_{2,2}$	$\phi_{2,3}$	$\phi_{2,4}$
A	0.9740953834	0.99447891278	0.9989095252
B	3.1897820557	3.0382130987	3.0073098797

To determine the accuracy of the approximations calculate

$$E_1(x) = 1 + xe^x - \phi_{2,2}(x)$$
$$E_2(x) = 1 + xe^x - \phi_{2,3}(x) \qquad (2.53)$$
$$E_3(x) = 1 + xe^x - \phi_{2,4}(x)$$

Calculations are carried out using MATLAB software and the code is provided in Appendix A2. Figure 2.3 shows the comparison of the ADM approximation values with exact values where there is no non-linear term. As it can be seen the difference between the ADM values and actual values is decreasing as the number of iterations, n, increases. The results show that the ADM results become more accurate and approaches the actual values as the number of terms increase.

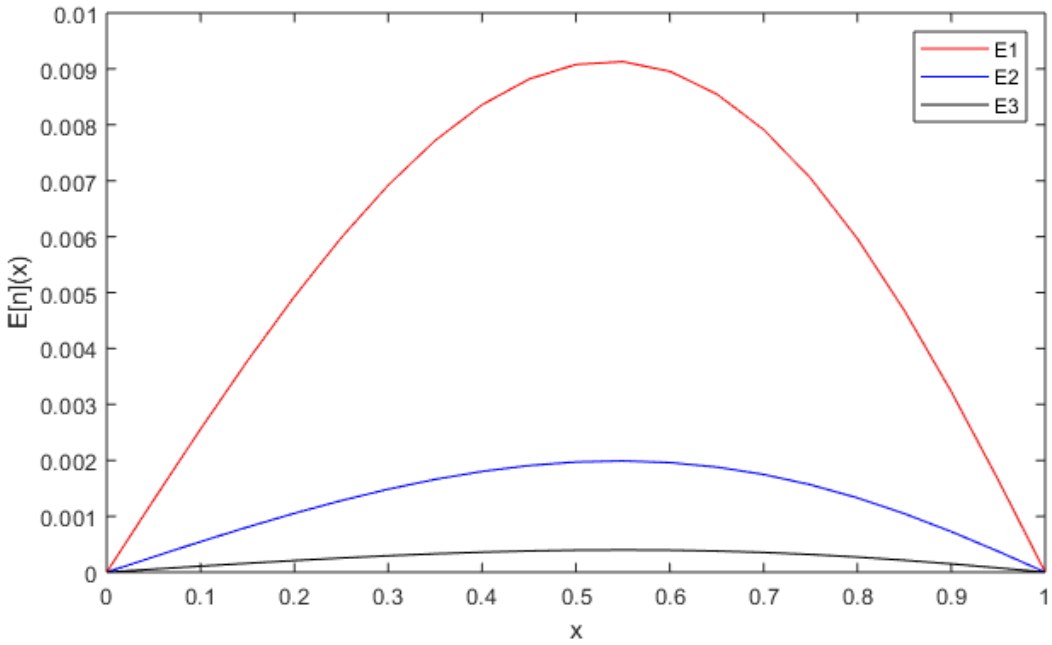

Figure 2.3 Error of ADM approximation value compared to actual value for linear BVP

2.3.2 Non-Linear Boundary Value Problem

Consider the non-linear fourth-order BVP of Eq. (2.40). On setting $f(x) = 1, \gamma = 0, g(x) = 0, h(x) = e^{-x}$ and $F(y) = y^2$ following is obtained

$$\frac{d^4y(x)}{dx^4} = 1 + \int_0^x e^{-x}y^2(x)\mathrm{d}x \quad 0 < x < 1 \tag{2.54}$$

subject to

$$y(0) = 1, y''(0) = 1, y(1) = e, y''(1) = e$$

The exact solution is

$$y = e^x \tag{2.55}$$

ADM decomposition algorithm can be written as follows

$$\begin{aligned} y_0 = &\quad 1 + Ax + x^2 + \frac{1}{3!}Bx^3 + G^{-1}(1) \\ y_{k+1} = &\; G^{-1}\left(\int_0^x e^{-x}A_k(x)\mathrm{d}x\right) \quad k \geq 0 \end{aligned} \tag{2.56}$$

where the constants $A = y'(0), B = y'''(0)$ are to be determined and the Adomian polynomials A_k are given as

$$A_0 = y_0^2(x), \;\; A_1 = 2y_0(x)y_1(x), \qquad \ldots$$

Again the truncated Taylor expansions for the exponential term is taken as in Eq. (2.50).

It should be observed how the accuracy is affected by these truncations. It can be shown that

$$\phi_{2,2}(x) = y_0 + G^{-1}(A_0) + G^{-1}(-xA_0)$$

$$\phi_{2,3}(x) = \phi_{2,2} + G^{-1}\left(\frac{x^2}{2}A_0\right) \tag{2.57}$$

$$\phi_{2,4}(x) = \phi_{2,3} + G^{-1}\left(-\frac{x^3}{6}A_0\right)$$

where

$$y_0 = 1 + Ax + \frac{1}{2}x^2 + \frac{B}{6}x^3 + \frac{1}{24}x^4$$

$$A_0 = 1 + 2Ax + (1 + A^2)x^2 + \left(\frac{B}{3} + A\right)x^3 + \left(\frac{1}{3} + \frac{AB}{3}\right)x^4 \tag{2.57}$$

$$+ \left(\frac{A}{12} + \frac{B}{6}\right)x^5 + \left(\frac{1}{24} + \frac{B^2}{36}\right)x^6 + \frac{B}{72}x^7 + \frac{1}{576}x^8$$

and A and B can be determined using the boundary conditions above and the results are provided in Table 2.2

Table 2.2 Values of A and B for non-linear BVP

	$\phi_{2,2}$	$\phi_{2,3}$	$\phi_{2,4}$
A	0.9969706142	1.0006029353	0.9998909027
B	1.0205416499	0.9960391622	1.0007021518

To determine the accuracy of the approximations the absolute error is calculated as

$$E_1(x) = \left|e^x - \phi_{2,2}(x)\right|$$

$$E_2(x) = \left|e^x - \phi_{2,3}(x)\right| \qquad (2.58)$$

$$E_3(x) = \left|e^x - \phi_{2,4}(x)\right|$$

Calculations are carried out using MATLAB software and the code is provided in Appendix A3. Figure 2.4 shows the absolute error of the ADM results with non-linear term present. As it can be seen the difference between the ADM values and actual values is decreasing as the number of terms, n, increases. The results show that the ADM works well with non-liner boundary value problem, too. Moreover, the ADM results with non-linear BVP gives more accurate results than those of linear BVP. This shows that ADM can be used to obtain reasonably accurate results with linear and especially with non-linear equations.

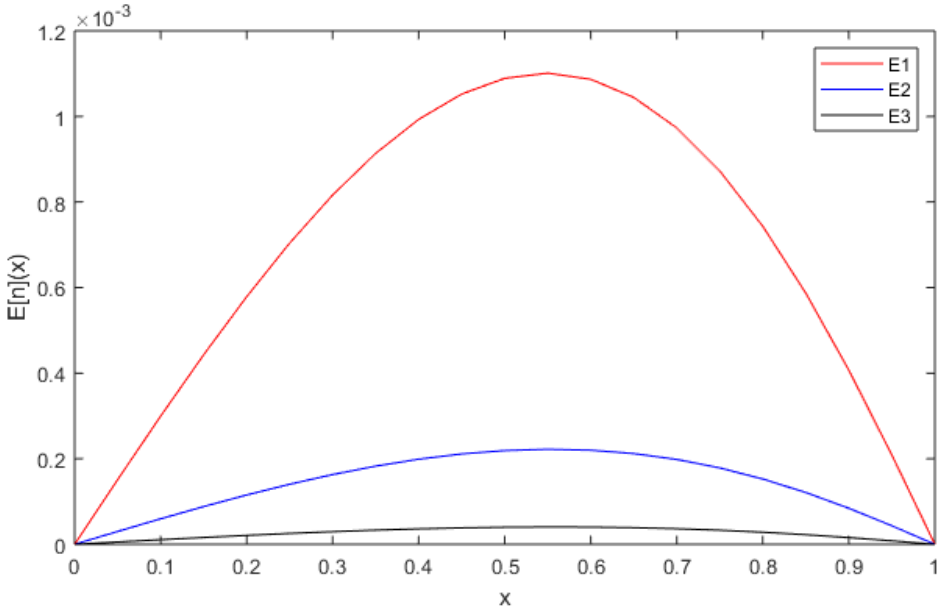

Figure 2.4 Error of ADM approximation value compared to actual value for nonlinear BVP

Chapter 3 – Adomian Modified Decomposition Method Applied to Various Foundation Types and Loadings Conditions

3.1 AMDM applied to Euler-Bernoulli beam and Winkler foundation with no loading

The governing equation for a uniform Euler-Bernoulli beam resting on a Winkler foundation is represented in Eq. (2.9). The Adomian Modified Decomposition Method (AMDM) will now be applied to solve this equation.

The AMDM states that, $\phi(X)$ in Eq. (2.39) can be represented as an infinite series, i.e.,

$$\phi(X) = \sum_{m=0}^{\infty} C_m X^m, \tag{3.1}$$

where the unknown coefficients, C_m, are determined recurrently. If a linear operator $G \equiv \mathrm{d}^4/\mathrm{d}X^4$ is used, then the inverse operator of G is a four-fold operator defined as

$$G^{-1} = \int_0^x \int_0^x \int_0^x \int_0^x (\cdots)\mathrm{d}X\mathrm{d}X\mathrm{d}X\mathrm{d}X. \tag{3.2}$$

Eq. (2.9) now can be written as

$$\phi(X) = \Phi(X) - G^{-1}\left\{-\frac{1}{2}\frac{\mathrm{d}^2\phi(X)}{\mathrm{d}X^2}\int_0^1\left(\frac{\mathrm{d}\phi(X)}{\mathrm{d}X}\right)^2 \mathrm{d}X + (K_0 - \lambda)\phi(X)\right\}. \tag{3.4}$$

where $\Phi(X)$ is a polynomial depending on the boundary conditions.

Eq. (3.4) contains a non-linear term which is referred to as the non-linear Fredholm integral coefficient. This term needs to be treated and simplified in order to use for the general solution method. Cauchy products are used to treat the non-linear term. First the term is re-written as

$$\frac{1}{2}\left(\int_0^1\left(\frac{\mathrm{d}\phi(X)}{\mathrm{d}X}\right)^2 \mathrm{d}X\right)\frac{\mathrm{d}^2\phi(X)}{\mathrm{d}X^2}. \tag{3.5}$$

Consider

$$\phi(X) = \sum_{m=0}^{\infty} C_m(X - X_0)^m. \tag{3.6}$$

By differentiating Eq. (3.6) then

$$\frac{\mathrm{d}\phi(X)}{\mathrm{d}X} = \sum_{m=0}^{\infty}(m+1)C_{m+1}(X - X_0)^m = \sum_{m=0}^{\infty} b_m(X - X_0)^m, \tag{3.7}$$

$$\frac{\mathrm{d}^2\phi(X)}{\mathrm{d}X^2} = \sum_{m=0}^{\infty}(m+1)\,(m+2)C_{m+2}(X - X_0)^m. \tag{3.8}$$

On setting $X_0 = 0$

$$\frac{\mathrm{d}^2\phi(X)}{\mathrm{d}X^2} = \sum_{m=0}^{\infty}(m+1)\,(m+2)C_{m+2}(X)^m = \sum_{m=0}^{\infty}\beta_m X^m. \tag{3.9}$$

The following can be obtained

$$\begin{aligned}\left(\frac{\mathrm{d}\phi(X)}{\mathrm{d}X}\right)^2 &= \left(\sum_{m=0}^{\infty} b_m(X-X_0)^m\right)\left(\sum_{l=0}^{\infty} b_l(X-X_0)^l\right)\\ &= \sum_{m=0}^{\infty} B_m(X-X_0)^m,\end{aligned} \tag{3.10}$$

where $B_m = \sum_{l=0}^{m} b_l b_{m-l}$.

After integrating the following is obtained

$$\begin{aligned}\frac{1}{2}\int_0^1 \left(\frac{\mathrm{d}\phi(X)}{\mathrm{d}X}\right)^2 \mathrm{d}X &= \frac{1}{2}\int_0^1 \sum_{m=0}^{\infty} B_m(X-X_0)^m \mathrm{d}X\\ &= \frac{1}{2}\sum_{m=0}^{\infty}\int_0^1 B_m(X-X_0)^m \mathrm{d}X = \left[\frac{1}{2}\sum_{m=0}^{\infty} B_m \frac{(X-X_0)^{m+1}}{m+1}\right]_{X=0}^{X=1}.\end{aligned} \tag{3.11}$$

By putting $X_0 = 0$ in the current analysis, one can obtain

$$\frac{1}{2}\int_0^1 \left(\frac{\mathrm{d}\phi(X)}{\mathrm{d}X}\right)^2 \mathrm{d}X = \sum_{m=0}^{\infty}\frac{B_m}{2(m+1)} = \sum_{m=0}^{\infty}\alpha_m. \tag{3.12}$$

Combining the results shown in Eq. (3.12) and Eq. (3.9) gives

$$\frac{1}{2}\left(\int_0^1 \left(\frac{d\phi(X)}{dX}\right)^2 dX\right)\frac{d^2\phi(X)}{dX^2} = \sum_{m=0}^{\infty}\alpha_m \sum_{l=0}^{\infty}\beta_l X^m$$
$$= \sum_{m=0}^{\infty} X^m \sum_{l=0}^{m}\alpha_l\beta_{m-l} = \sum_{m=0}^{\infty}\zeta_m X^m, \tag{3.13}$$

where

$$\zeta_m = \sum_{l=0}^{m}\alpha_l\beta_{m-l}. \tag{3.14}$$

Now the treated non-linear term needs to be combined back into Eq. (3.4) with application of $\phi(X) = \sum_{m=0}^{\infty} C_m X^m$. The following is obtained

$$\phi(X) = \Phi(X) + G^{-1}\left\{\sum_{m=0}^{\infty}\zeta_m X^m - (K_0 - \lambda)\sum_{m=0}^{\infty} C_m X^m\right\} \tag{3.15}$$

3.1.1 Solution algorithm

In Eq. (3.15) the initial term $\Phi(X)$ can be represented as

$$\Phi(X) = \sum_{m=0}^{3} C_m X^m$$
$$= \phi(0) + \phi'(0)X + \phi''(0)\,X^2/2 + \phi'''(0)\,X^3/6 \tag{3.16}$$

From this one can obtain a recurrence relation of C_m as follows

$$C_0 = \phi(0), \qquad C_1 = \phi'(0), \qquad C_2 = \frac{\phi''(0)}{2}, \quad C_3 = \frac{\phi'''(0)}{6} \tag{3.17}$$

for $m \geq 4$

$$C_m = \frac{1}{m(m-1)(m-2)(m-3)} \sum_{j=0}^{m-4} [\zeta_j - (K_0 - \lambda)C_j] \qquad (3.18)$$

The coefficients C_m is determined from the recurrence Eqs. (3.17) and (3.18) and the solution for $\phi(X)$ calculated using Eq. (3.15). The series solution is $\phi(X) = \sum_{m=0}^{\infty} C_m X^m$, although not all of the coefficients C_m can be determined. The solutions must be approximated by the truncated series $\sum_{m=0}^{n-1} C_m X^m$. The successive approximations are $\phi^{[n]}(X) = \sum_{m=0}^{n-1} C_m X^m$, by increasing n until the boundary conditions are met.

Thus, $\phi^{[1]}(X) = C_0$, $\phi^{[2]}(X) = \phi^{[1]}(X) + C_1 X$, $\phi^{[3]}(X) = \phi^{[2]}(X) + C_2 X^2$, $\phi^{[4]}(X) = \phi^3(X) + C_3 X^3$ serve as approximate solutions with increasing accuracy as $n \to \infty$. The four coefficients $C_m (m = 0,1,2,3)$ in eq. (3.17) depend on the boundary conditions of Eq. (2.20). The two coefficients C_0 and C_1 are chosen as arbitrary constants, and the other two coefficients C_2 and C_3 are expressed as functions of C_0 and C_1. Thus from Eq. (2.20) and Eq. (3.17) one can obtain the following

$$C_2 = \frac{\kappa_{L0}}{2} C_1, \quad C_3 = -\frac{\kappa_{Ro}}{6} C_0 \qquad (3.19)$$

Thus the initial term $\Phi(X)$ can be represented as a function of C_0 and C_1 and from the Eq. (3.19) the coefficients $C_m (m \geq 4)$ are functions of C_0, C_1 and λ. By substituting $\phi^{[n]}(X)$ into the boundary conditions of Eq. (2.20) when $X = 1$, following is obtained

$$f_{r0}^{[n]}(\lambda)C_0 + f_{r1}^{[n]}(\lambda)C_1 = 0, \;\; r = 1,2 \tag{3.20}$$

For non-trivial solutions, C_0 and $C_1$the frequency equation is expressed as

$$\begin{vmatrix} f_{10}^{[n]}(\lambda) & f_{11}^{[n]}(\lambda) \\ f_{20}^{[n]}(\lambda) & f_{21}^{[n]}(\lambda) \end{vmatrix} = 0 \tag{3.21}$$

The i^{th} estimated eigenvalue $\lambda_{(i)}^{[n]}$ corresponding to m is obtained from Eq. (3.21), i.e., the i^{th} estimated dimensionless natural frequency $\Omega_{n(i)}^{[n]} = \sqrt{\lambda_{(i)}^{[n]}}$ is also obtained and n is determined by

$$\left|\Omega_{n(i)}^{[n]} - \Omega_{n(i)}^{[n-1]} \leq \varepsilon\right| \tag{3.22}$$

where $\Omega_{n(i)}^{[n-1]}$ is the i^{th} estimated dimensionless natural frequency corresponding to $n-1$, and ε is a pre-set sufficiently small value. By substituting $\Omega_{n(i)}^{[n]}$ into Eq. (3.20) then

$$C_1 = -\frac{f_{r0}^{[n]}\left(\Omega_{n(i)}^{[n]}\right)}{f_{r1}^{[n]}\left(\Omega_{n(i)}^{[n]}\right)}C_0, \;\; r = 1,2 \tag{3.23}$$

and other coefficients C_m can be calculated from Eqs. (3.18) and (3.19). The i^{th} mode shape $\phi_i^{[n]}$corresponding to the i^{th} eigenvalue $\Omega_{n(i)}^{[n]}$is obtained using

$$\phi_i^{[n]}(X) = \sum_{m=0}^{n-1} C_m^{[i]} X^m \tag{3.23}$$

where $\phi_i^{[n]}$ is the i^{th} eigenfunction corresponding to the i^{th} eigenvalue λ_i, and $C_m^{[i]}(X)$ is $C_m(X)$ in which λ is substituted by λ_i. By normalizing Eq. (3.23) the i^{th} normalised eigenfunction is obtained by

$$\bar{\phi}_i^{[n]}(X) = \frac{\phi_i^{[n]}(X)}{\sqrt{\int_0^1 \left[\phi_i^{[n]}(X)\right]^2 \mathrm{d}X}} \tag{3.24}$$

where $\bar{\phi}_i^{[n]}(X)$is the i^{th} mode shape function of the beam corresponding to the i^{th} natural frequency $\omega_i^{[n]} = \sqrt{\lambda_i^{[n]}}\sqrt{EI/\rho A l^4} = \Omega_{n(i)}^{[n]}\sqrt{EI/\rho A l^4}$.

This general theory can now be used to analyze a beam vibration frequencies with different boundary conditions.

Clamped-Clamped Uniform Beam boundary conditions were chosen to investigate the vibration of the Euler-Bernoulli beam resting on a Winker foundation without any loading. Clamped-Clamped boundary condition was chosen due to its better physical representation of railway track beam compared to other boundary conditions. Boundary conditions for this case are given in Eqs. (2.19) and (2.20) and the spring constants leading to, $\kappa_{L0} \to \infty, \kappa_{R0} \to \infty, \kappa_{L1} \to \infty, \kappa_{R1} \to \infty$.

When $X = 0$ the first two boundary conditions of Eq. (2.20) give the relationships shown in Eq. (3.20) and when $X = 1$ by substituting $\phi^{[n]}(X) = \sum_{m=0}^{n-1} C_m X^m$ into the last two boundary conditions of Eq. (2.20) the following two algebraic equations involving C_1 and C_0 can be obtained

$$\sum_{m=0}^{n-1} C_m = f_{11}^{[n]}(\lambda)C_0 + f_{12}^{[n]}(\lambda)C_1 = 0$$
$$\sum_{m=0}^{n-2} (m+1)C_{m+1} = f_{21}^{[n]}(\lambda)C_0 + f_{22}^{[n]}(\lambda)C_1 = 0 \quad (3.25)$$

Now Eq. (3.25) can be solved using Eq. (3.21) and further numerical results are calculated.

3.1.2 Results

Natural frequencies $\Omega_{n(i)}$ were calculated for the first three modes using four different foundation stiffness values. Calculations were performed in MATLAB software and the code is provided in Appendix A5. Table 3.1 shows the results of frequencies involving the nonlinear term in Eq. (3.15). From the Table 3.1 it can be seen that frequencies increase as the value of stiffness of the foundation increases. This trend is also observed with the increase of number of modes.

Table 3.1 Natural frequencies of beam on Winkler foundation for different K_0

Natural Frequencies	$K_0 = 0$	$K_0 = 1$	$K_0 = 5$	$K_0 = 100$
$\Omega_{n(1)}$	4.8406	4.9428	5.3321	11.11
$\Omega_{n(2)}$	9.7671	9.8182	10.02	13.978
$\Omega_{n(3)}$	12.241	12.282	12.443	15.806

Table 3.2 compares the results calculated with the non-linear term in Eq. (3.15) present to the result when it was absent for $K_0 = 1$. Here $\Omega_{non(i)}$ denotes

natural frequencies with non-linear term present, and $\Omega_{n(i)}$ denotes natural frequencies without non-linear term. From the ratio of the results it can be noticed that the presence of the non-linear term quite significantly increases the natural frequencies and also the ratio grows with the increase of the number of modes.

Table 3.2 Natural frequencies of beam on Winkler foundation with and without nonlinear term for $K_0 = 1$

Modes	$\Omega_{n(i)}$	$\Omega_{non(i)}$	$\Omega_{non(i)} / \Omega_{n(i)}$
1	4.5937	4.9428	1.076
2	9.0741	9.8182	1.082
3	11.1351	12.282	1.103

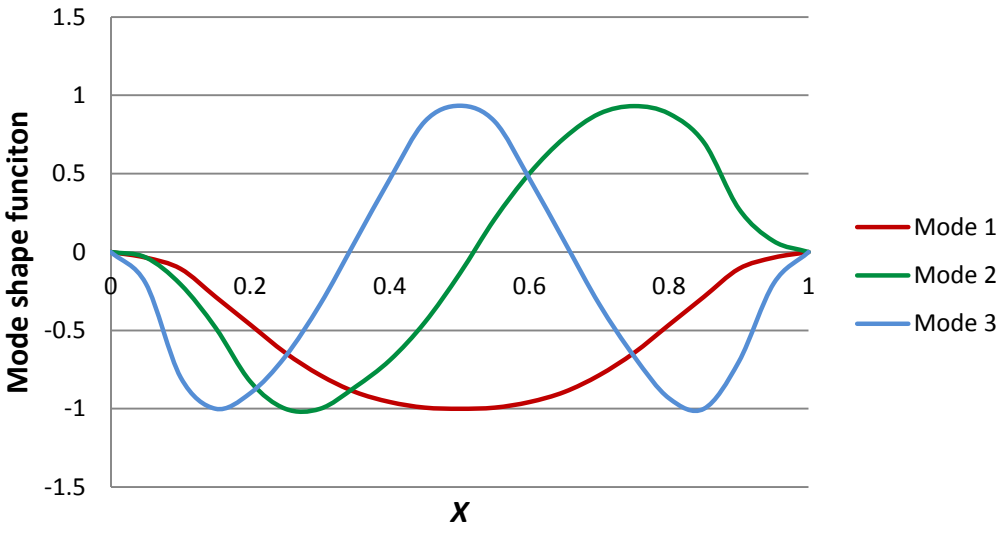

Figure 3.1 Mode shapes for the first thee modes when $K_0 = 5$

Calculated natural frequencies now substituted back into Eq. (3.23) and (3.24) to obtain polynomials to describe the mode shape functions. Fiqure 3.1

represents the first three mode shapes for clamped-clamped beam on Winkler foundation when the stiffness parameter $K_0 = 5$.

Figure 3.2 shows the convergence of natural frequencies of the first three modes. The method gives fast convergence especially for the first mode which gives an accurate result after only $n = 8$. Although it fluctuates a lot at the beginning, the results for the second mode are also quite accurate after 12 iterations. For the third mode it took longer to converge, after about 15 iterations.

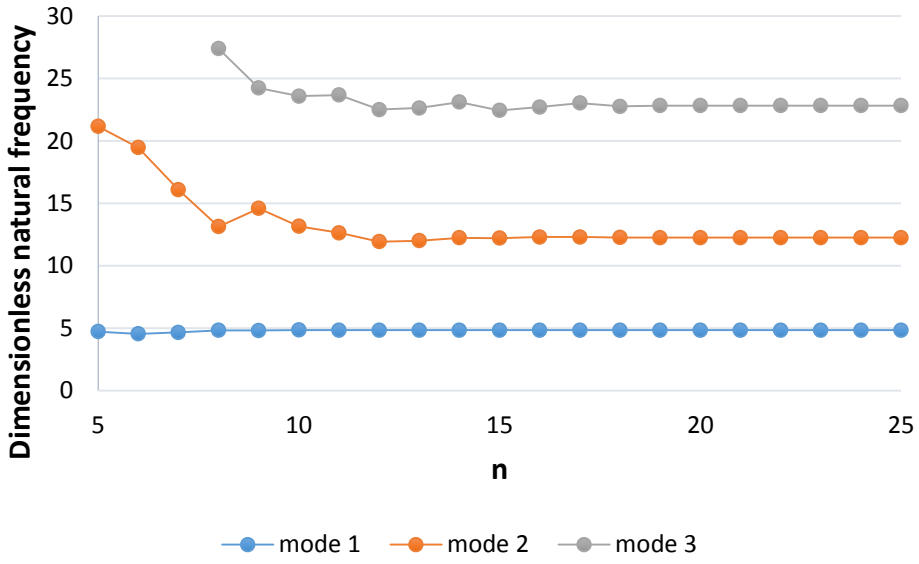

Figure 3.2 Convergence of natural frequencies for $K_0 = 1$

3.2 AMDM applied to Euler-Bernoulli beam and Winkler foundation with harmonic non-moving loading

The case considered in section 3.1, the Euler-Bernoulli beam resting on Winkler foundation, is now investigated under harmonic non-moving loading. In

order to apply AMDM the expression describing the loaded beam is formulated first.

3.2.1 Mathematical formulation

Beam element motion can be expressed by following equations [29]

$$\frac{\partial V}{\partial x} + q(x,t) - k_w w(x,t) = \rho A \frac{\partial^2 w}{\partial t^2}, \tag{3.31}$$

$$V(x,t) - \frac{\partial M}{\partial x} = \rho I \frac{\partial^2 \theta}{\partial t^2} \tag{3.32}$$

The relations of the slope-deflection and force-displacement is represented as followings

$$\theta = \frac{\partial w}{\partial x} \quad \text{and} \quad M(x,t) = -EI \frac{\partial^2 w}{\partial t^2} \tag{3.33}$$

where θ is the rotation and $M(x,t)$ is the bending moment. Substitute Eq. (3.32) and Eq. (3.33) into Eq. (3.31), and following lateral response equation is obtained.

$$EI \frac{\partial^4 w(x,t)}{\partial x^4} - \rho I \frac{\partial^4 w(x,t)}{\partial x^2 \partial t^2} + k_w w(x,t) + \rho A \frac{\partial^2 w(x,t)}{\partial t^2} = q(x,t) \tag{3.34}$$

Using Eq. (2.5) the eigenvalue problem of Eq. (3.34) reduces to

$$EI\frac{\mathrm{d}^4\phi(x)}{\mathrm{d}x^4}+\rho I\omega^2\frac{\mathrm{d}^2\phi(x)}{\mathrm{d}x^2}+k_w\phi(x)-\rho A\omega^2\phi(x)=q(x) \tag{3.35}$$

Eq. (3.35) is now made non-dimensional using

$$X=\frac{x}{l},\ \ \phi(X)=\frac{\phi(x)}{l},\qquad K_0=\frac{k_w l^4}{EI},\ \ \lambda=\frac{\rho A\omega^2 l^4}{EI},\qquad \gamma=l^2\frac{A}{I}$$

and becomes

$$\frac{\mathrm{d}^4\phi(X)}{\mathrm{d}X^4}+\frac{\lambda}{\gamma}\frac{\mathrm{d}^2\phi(X)}{\mathrm{d}x^2}+(K_0-\lambda)\phi(X)=\frac{L^3q(X)}{EI} \tag{3.36}$$

3.2.2 Discontinuous load expansion

Concentrated discontinuous load can be turned into continuous function using Fourier Expansion.

$$q(x)=\sum_{n=1}^{N_1}q_m\sin\frac{m\pi x}{L} \tag{3.37}$$

By multiplying both sides of equation (3.37) by $\sin\frac{m\pi x}{L}$ and integrating

$$\int_0^L q(x)\sin\frac{n\pi x}{L}=\int_0^L q_n\sin\frac{n\pi x}{L}\sin\frac{n\pi x}{L}\,dx \tag{3.38}$$

Using the trigonometric function orthogonality property,

$$\int_0^1 \sin m\pi X \sin n\pi X \, dX = 0 \quad \text{for} \quad n \neq m$$

$$\int_0^1 \sin m\pi X \sin n\pi X \, dX = \frac{L}{2} \quad \text{for} \quad n = m \tag{3.39}$$

Using this property, the continuous load amplitude is expressed as

$$q_n = \frac{2}{L} \int_0^1 q(X) \sin n\pi X \, dX \tag{3.40}$$

This can be applied for the concentrated load by assuming that load is distributed over an infinitesimal interval δ

$$q_n = \frac{2q}{\delta L} \int_{X_1 - \frac{\delta}{2}}^{X_1 + \frac{\delta}{2}} \sin n\pi X \, dX = \frac{4q}{n\pi\delta L} \left(\sin n\pi X \sin \frac{n\pi\delta}{2} \right) \tag{3.41}$$

As $\delta \to 0$, $\sin \frac{n\pi\delta}{2} \cong \frac{n\pi\delta}{2}$, therefore

$$q_n = \frac{2q}{L} \sin n\pi X \tag{3.42}$$

Substituting Eq. (3.42) into Eq. (3.38) and making non-dimensional using

$$Q = \frac{qL^3}{EI}$$

and Eq. (3.37) becomes

$$Q(X) = \sum_{n=1}^{N_1} Q_n \sin n\pi X \tag{3.43}$$

where $Q_n = 2Q \sin n\pi X$

Finally Eq. (3.36) becomes non-dimensional throughout by substituting Eq. (3.43)

$$\frac{\mathrm{d}^4\phi(X)}{\mathrm{d}X^4} + \frac{\lambda}{\gamma}\frac{\mathrm{d}^2\phi(X)}{\mathrm{d}x^2} + (K_0 - \lambda)\phi(X) = Q(X) \tag{3.37}$$

3.2.3 Application of the AMDM

AMDM can now be applied for Eq. (3.37) following the same procedure as described in section 3.1

$$\phi(X) = \Phi(X) +$$

$$+G^{-1}\left\{-\frac{\lambda}{\gamma}\frac{\mathrm{d}^2\phi(X)}{\mathrm{d}x^2} - (K_0 - \lambda)\phi(X) + \sum_{n=1}^{N_1} Q_n \sin n\pi X\right\} \tag{3.38}$$

The last term of Eq. (3.38) is solved by simple integration,

$$\sum_{n=1}^{N_1} Q_n \int_0^x \int_0^x \int_0^x \int_0^x (\sin n\pi X)\mathrm{d}X\mathrm{d}X\mathrm{d}X\mathrm{d}X$$

$$= \sum_{n=1}^{N_1} Q_n \left(\frac{\sin n\pi X}{(n\pi)^4} - \frac{X}{(n\pi)^3} + \frac{X^3}{3!\,(n\pi)}\right) \tag{3.39}$$

and now Eq. (3.38) becomes

$$\phi(X) = \Phi(X) + \sum_{n=1}^{N_1} Q_n \left(\frac{\sin n\pi X}{(n\pi)^4} - \frac{X}{(n\pi)^3} + \frac{X^3}{3!\,(n\pi)} \right) + G^{-1} \left\{ -\frac{\lambda}{\gamma} \frac{\mathrm{d}^2 \phi(X)}{\mathrm{d}x^2} - (K_0 - \lambda)\phi(X) \right\} \tag{3.40}$$

By substituting $\phi(X) = \sum_{m=0}^{\infty} C_m X^m$, and its second derivatives into Eq. (3.40) one can obtain

$$\phi(X) = \Phi(X) + \sum_{n=1}^{N_1} Q_n \left(\frac{\sin n\pi X}{(n\pi)^4} - \frac{X}{(n\pi)^3} + \frac{X^3}{3!\,(n\pi)} \right) + G^{-1} \left\{ -\frac{\lambda}{\gamma} \sum_{m=0}^{\infty} (m+1)(m+2) C_{m+2} X^m - (K_0 - \lambda) \sum_{m=0}^{\infty} C_m X^m \right\} \tag{3.41}$$

Recurrence relation for the first 4 terms of coefficients C_m can be written as in Eq. (3.17) and for $m \geq 4$ as

$$C_m = \frac{1}{m(m-1)(m-2)(m-3)} \sum_{j=0}^{m-4} \left[-\frac{\lambda}{\gamma} (j+1)(j+2) C_{j+2} - (K_0 - \lambda) C_j \right] \tag{3.42}$$

Vibration response of Euler-Bernoulli beam resting on Winkler foundation under harmonic non-moving loading is now calculated using

Clamped-Free Uniform Beam boundary conditions where the spring constants becoming, $\kappa_{L0} \to \infty, \kappa_{R0} \to 0, \kappa_{L1} \to \infty, \kappa_{R1} \to 0$.

Algebraic equation arising from boundary conditions in Eq. (2.19) and (2.20) with $X = 0$ and $X = 1$ will be as follows using the same method described in section 3.1

$$\sum_{m=0}^{n-3}(m+1)(m+2)C_{m+2} + \kappa_{R0}\sum_{m=0}^{n-2}(m+1)C_{m+1} = f_{11}^{[n]}(\lambda)C_0 + f_{12}^{[n\}}(\lambda)C_1 = 0$$

$$\sum_{m=0}^{n-4}(m+1)(m+2)(m+3)C_{m+3} - \kappa_{R1}\sum_{m=0}^{n-1}C_m = f_{21}^{[n]}(\lambda)C_0 + f_{22}^{[n]}(\lambda)C_1 = 0 \tag{3.43}$$

Eq. (3.42) will be used to define the coefficients for solving the Eq. (3.43).

3.2.4 Results

Numerical results for the frequencies were obtained using four different foundation stiffness parameters. The code used for calculations are provided in Appendix A5. The results are tabulated in table 3.3. It can be seen that with beam subjected to concentrated loading shows similar pattern as unloaded beam. However, the overall frequencies of loaded beam for all modes and foundation parameters are smaller compared to those of free vibrating beam. Increase of the

stiffness parameter also increases the frequency. However, the change is negligible until the stiffness parameter becomes significant.

Table 3.3 Frequencies of beam on an elastic foundation for different K_0

Frequencies	$K_0 = 0$	$K_0 = 5$	$K_0 = 50$	$K_0 = 1000$
$\Omega_{n(1)}$	2.3298	2.5311	3.6209	5.8945
$\Omega_{n(2)}$	5.5724	5.6117	6.0859	7.8393
$\Omega_{n(3)}$	7.7353	7.7515	7.9475	11.27

By substituting obtained $\Omega_{n(1)}$ back into Eqs. (3.42) and (3.23) and normalizing it using Eq. (3.24), a polynomial is derived that describes the first mode shape function. Other natural frequencies modes shapes are obtained in the same way. Figure 3.3 and Figure 3.4 illustrates the first and the third mode shape functions of frequencies, respectively, and the effect of different elastic stiffness on the shape. It can be seen that stiffness parameter does not change the mode shapes much. However, at large values of K_0 the change of shapes are significant and it can be noticed that amplitude of third mode shape greatly changes.

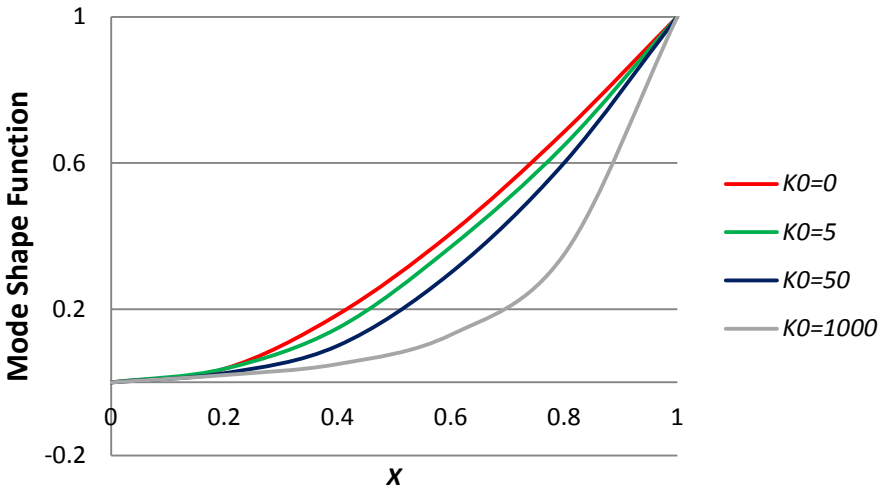

Figure 3.3 Variation of first mode shape for different K_0

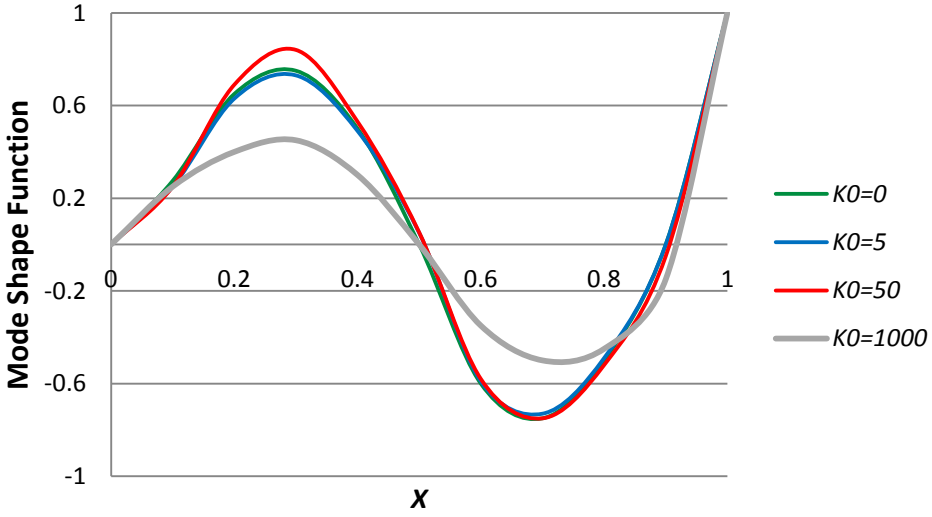

Figure 3.4 Variation of third mode shape for different K_0

The convergence of results for beam under harmonic non-moving loading is provided in Figure 3.5. Again the AMDM provides fast and accurately converged results, although it took longer for 2nd and third modes. It can be observed that there is an excellent convergence for the first mode only after 10

iterations, however the third mode results fluctuated until it gets steady at $n = 18$.

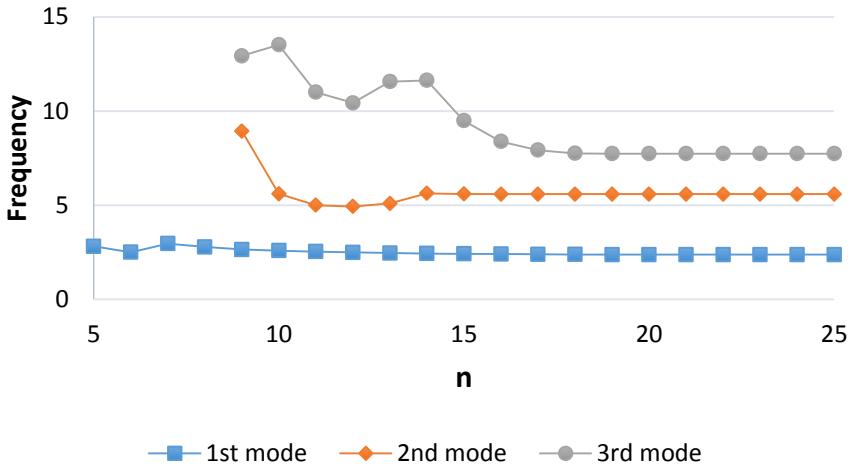

Figure 3.5 Convergence of frequencies for $K_0 = 1$

3.3 AMDM applied to Euler-Bernoulli beam and Pasternak foundation with harmonic high-speed moving loading

Governing forth order equation describing Euler Bernoulli beam resting on two parameter Pasternak foundation is formulated. AMDM is applied for the equation. Obtained expression then combined with the moving loading by substituting it to the right hand sight of the equation.

3.3.1 Mathematical formulation

By introducing shear parameter Eq. (3.31) becomes

$$\frac{\partial V}{\partial x} + q(x,t) - k_w w(x,t) + k_p \frac{\partial^2 w}{\partial t^2} = \rho A \frac{\partial^2 w}{\partial t^2}, \qquad (3.44)$$

where $q(x,t)$ is lateral excitation, k_w and k_p are the linear and shear stiffness of foundation. Substitute Eq. (3.32) and Eq. (3.33) into Eq. (3.44), and following lateral response equation is obtained

$$EI\frac{\partial^4 w(x,t)}{\partial x^4} - k_p\frac{\partial^2 w}{\partial t^2} - \rho I\frac{\partial^4 w(x,t)}{\partial x^2 \partial t^2} + k_w w(x,t) + \rho A\frac{\partial^2 w(x,t)}{\partial t^2} = q(x,t) \tag{3.45}$$

Using Eq. (2.5) the eigenvalue problem of Eq. (3.45) reduces to

$$EI\frac{\mathrm{d}^4\phi(x)}{\mathrm{d}x^4} + k_p\omega^2\phi(x) + \rho I\omega^2\frac{\mathrm{d}^2\phi(x)}{\mathrm{d}x^2} + k_w\phi(x) - \rho A\omega^2\phi(x) = q(x) \tag{3.46}$$

Eq. (3.46) is now made non-dimensional using

$$X = \frac{x}{l},\ \ \phi(X) = \frac{\phi(x)}{l}, \qquad K_0 = \frac{k_w l^4}{EI}, \qquad K_1 = \frac{k_p l^2}{EI} \quad \lambda = \frac{\rho A\omega^2 l^4}{EI},$$

$$\gamma = l^2\frac{A}{I}, Q = \frac{qL^3}{EI}$$

and becomes

$$\frac{\mathrm{d}^4\phi(X)}{\mathrm{d}X^4} + \left(\frac{\lambda}{\gamma} - K_1\right)\frac{\mathrm{d}^2\phi(X)}{\mathrm{d}x^2} + (K_0 - \lambda)\phi(X) = Q(X) \tag{3.47}$$

3.3.2 Distributed harmonic high-speed moving loading

Now consider the model of a train consisting of a few wagons. Loading generated by wagons can be represented by a finite sum of harmonically varying loads and formulated as follows using Heaviside function,

$$q(x,t) = \sum_{d=0}^{D-1} \frac{P_0}{2r} cos^2\left(\frac{\pi(x - vt - (2r+s)d)}{2r}\right) * H(r^2 - (x - vt - (2r+s)d)^2)e^{i\Omega t} \tag{3.48}$$

where P_0 is the load, $2r$ is the span of the load, $H(:)$ is the Heaviside function, v the velocity of moving load, $\Omega = 2\pi f_\Omega$ frequency of the moving load, D is a number of separated impulses and s is the distance between them.

Figure 3.6 and 3.7 represents the load distribution of a train consisting of a few wagons, moving along a beam. The function was calculated for different impulse numbers and frequency values (Appendix A4).

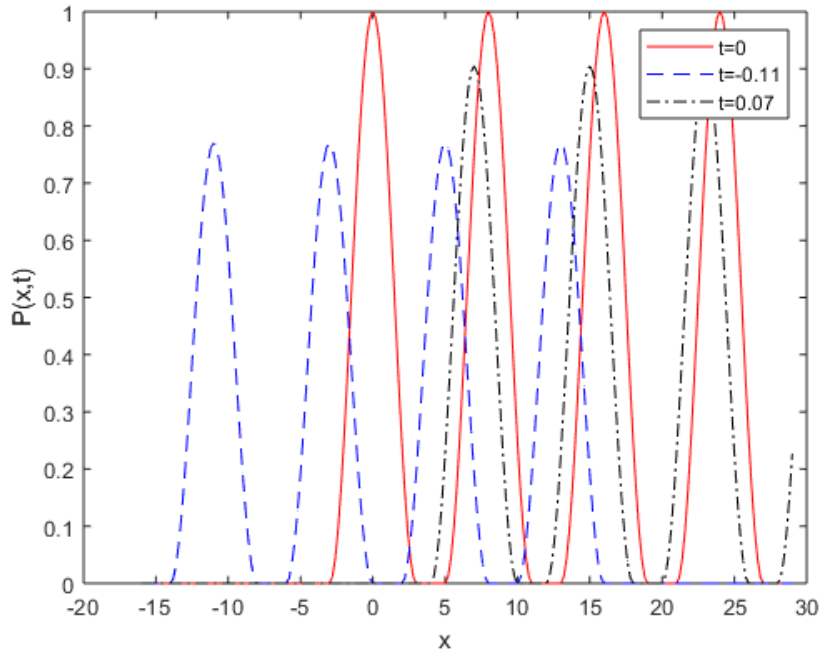

Figure 3.6 A series of distributed harmonic loads for v=100m/s, D=4 and f=1

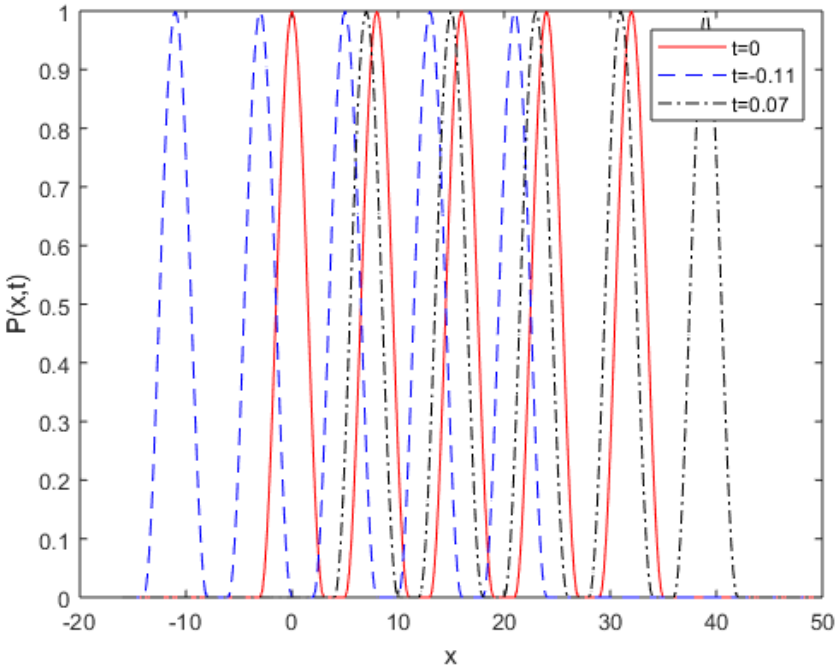

Figure 3.7 A series of distributed harmonic loads for v=100m/s, D=5 and f=0

Eq. (3.48) is made non-dimensional using

$$X = \frac{x}{l}, R = \frac{r}{l}, V = \frac{v}{l}, S = \frac{s}{l}$$

and becomes

$$Q(X,t) = \sum_{d=0}^{D-1} \frac{P_0}{2R} cos^2\left(\frac{\pi(X - Vt - (2R+S)d)}{2r}\right) \\ * H(R^2 - (X - Vt - (2R+S)d)^2) e^{i\Omega t} \tag{3.49}$$

By substituting Eq.(3.49) to the r.h.s of the Eq. (3.47) one can obtain

$$\frac{\mathrm{d}^4\phi(X)}{\mathrm{d}X^4} + \left(\frac{\lambda}{\gamma} - K_1\right)\frac{\mathrm{d}^2\phi(X)}{\mathrm{d}x^2} + (K_0 - \lambda)\phi(X) \\ = \sum_{d=0}^{D-1} \frac{P_0}{2R} cos^2\left(\frac{\pi(X - Vt - (2R+S)d)}{2R}\right) \\ * H(R^2 - (X - Vt - (2R+S)d)^2) e^{i\Omega t} \tag{3.50}$$

3.3.3 Application of the AMDM

AMDM can now be applied for Eq. (3.50) following the same procedure as described in section 3.1

$$\phi(X) = \Phi(X) \\ + G^{-1}\left\{\left(K_1 - \frac{\lambda}{\gamma}\right)\frac{\mathrm{d}^2\phi(X)}{\mathrm{d}x^2} - (K_0 - \lambda)\phi(X)\right. \\ + \sum_{d=0}^{D-1} \frac{P_0}{2R} cos^2\left(\frac{\pi(X - Vt - (2R+S)d)}{2R}\right) \\ \left. * H(R^2 - (X - Vt - (2R+S)d)^2)\right\} \tag{3.51}$$

By substituting $\phi(X) = \sum_{m=0}^{\infty} C_m X^m$, and its second derivative into Eq. (3.51) one can obtain

$$\begin{aligned}\phi(X) &= \Phi(X) \\ &+ G^{-1}\left\{\left(K_1 - \frac{\lambda}{\gamma}\right)\sum_{m=0}^{\infty}(m+1)(m+2)C_{m+2}X^m\right. \\ &- (K_0 - \lambda)\sum_{m=0}^{\infty} C_m X^m \\ &+ \sum_{d=0}^{D-1}\frac{P_0}{2R}cos^2\left(\frac{\pi(X - Vt - (2R+S)d)}{2R}\right)H(R^2 \\ &\left.- (X - Vt - (2R+S)d)^2)\right\}\end{aligned} \tag{3.52}$$

The first 4 terms of coefficients C_m are as in Eq. (3.17) and C_m for $m \geq 4$ as following

$$\begin{aligned}C_m = \frac{1}{m(m-1)(m-2)(m-3)}\sum_{j=0}^{m-4}\left[\left(K_1 - \frac{\lambda}{\gamma}\right)(j+1)(j\right. \\ \left.+2)C_{j+2} - (K_0 - \lambda)C_j\right]\end{aligned} \tag{3.53}$$

Vibration response of the Euler-Bernoulli beam resting on the Pasternak foundation is now calculated using Clamped-Free boundary conditions where the spring constants becoming, $\kappa_{L0} \to \infty, \kappa_{R0} \to 0, \kappa_{L1} \to \infty, \kappa_{R1} \to 0$ as per Eqs. (2.19) and (2.20).

Algebraic equation arising from boundary conditions in Eq. (2.19) and (2.20) with $X = 0$ and $X = 1$ will be as follows using the same method described in section 3.1

$$\sum_{m=0}^{n-3}(m+1)(m+2)C_{m+2} + \kappa_{R0}\sum_{m=0}^{n-2}(m+1)C_{m+1} = f_{11}^{[n]}(\lambda)C_0 + f_{12}^{[n\}}(\lambda)C_1 = 0$$

$$\sum_{m=0}^{n-4}(m+1)(m+2)(m+3)C_{m+3} - \kappa_{R1}\sum_{m=0}^{n-1}C_m = f_{21}^{[n]}(\lambda)C_0 + f_{22}^{[n]}(\lambda)C_1 = 0 \tag{3.54}$$

Eq. (3.53) will be used to define the coefficients for solving the Eq. (3.54).

3.3.4 Results

Table 3.4 provides the results of frequencies of first three modes of a beam vibration subjected to harmonic moving loading for different Pasternak parameters, K_1 while keeping stiffness, K_0 constant. The overall pattern is similar with those of section 3.2. The effect of the stiffness parameter on beam vibration frequency in presence of the constant shear parameter was also analysed and the numerical results are provided in Table 3.5. from the last columns of Table 3.4 and Table 3.5 in can be noticed that the frequency is influenced the most in by $K_1 = 1000$ in Table 3.4. From this it can be

concluded that the shear parameter has greater effect for the beam vibration frequency compared to the stiffness parameter.

Table 3.4 Frequencies of beam on an elastic foundation for different K_1 with $K_0 = 1$

Frequencies	$K_1 = 0$	$K_1 = 5$	$K_1 = 50$	$K_1 = 1000$
$\Omega_{n(1)}$	2.3721	3.1009	5.3574	27.942
$\Omega_{n(2)}$	5.58	5.9769	8.8382	31.061
$\Omega_{n(3)}$	7.7385	8.0402	10.388	35.199

Table 3.5 Frequencies of beam on an elastic foundation for different K_0 with $K_1 = 1$

Frequencies	$K_0 = 0$	$K_0 = 5$	$K_0 = 50$	$K_0 = 1000$
$\Omega_{n(1)}$	2.4954	2.6859	3.7419	5.978
$\Omega_{n(2)}$	5.654	5.6921	6.1553	7.9019
$\Omega_{n(3)}$	7.7966	7.8125	8.0045	11.315

This effect can also be observed in Figures 3.8 and 3.9 where the frequency at each phase and with changing particular parameter is compared to the initial frequency where its foundation parameter equals zero. Even though comparison was performed only until $K_0 = 15$ and $K_1 = 15$, it can be noticed that overall ratio of any mode in Figure 3.8, where shear parameter is varied keeping stiffness constant, is greater than in Figure 3.9, where the stiffness is varied keeping the shear constant. Moreover, both figures show that the first mode is the most affected by any parameter than other modes.

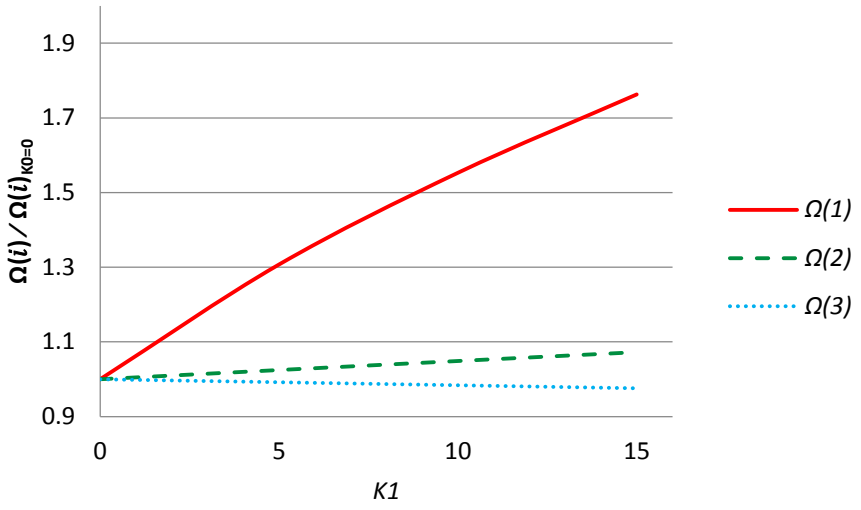

Figure 3.8 The effect of the foundation stiffness K_1 to frequencies, at $K_0 = 1$

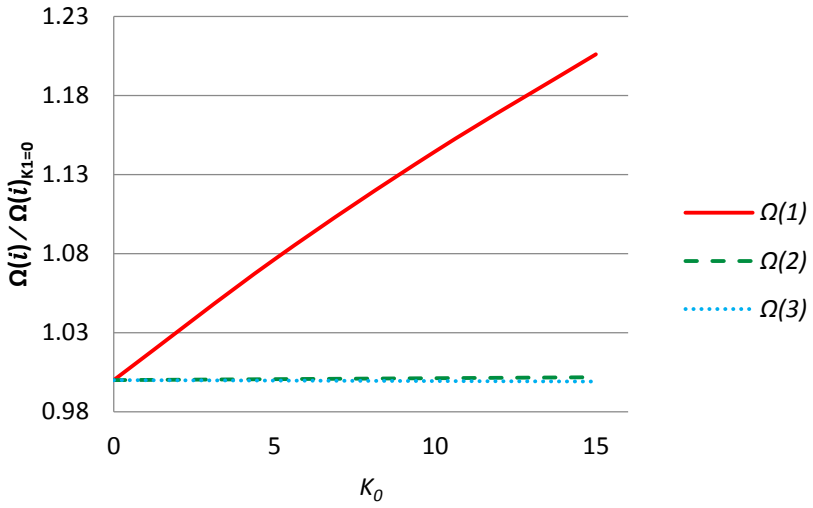

Figure 3.9 The effect of the foundation stiffness K_0 to frequencies, at $K_1 = 1$.

Again good convergence of obtained results of beam vibration frequencies on Pasternak foundation can be seen from Figure 3.10 where the first three modes successfully converge after about 16 iterations.

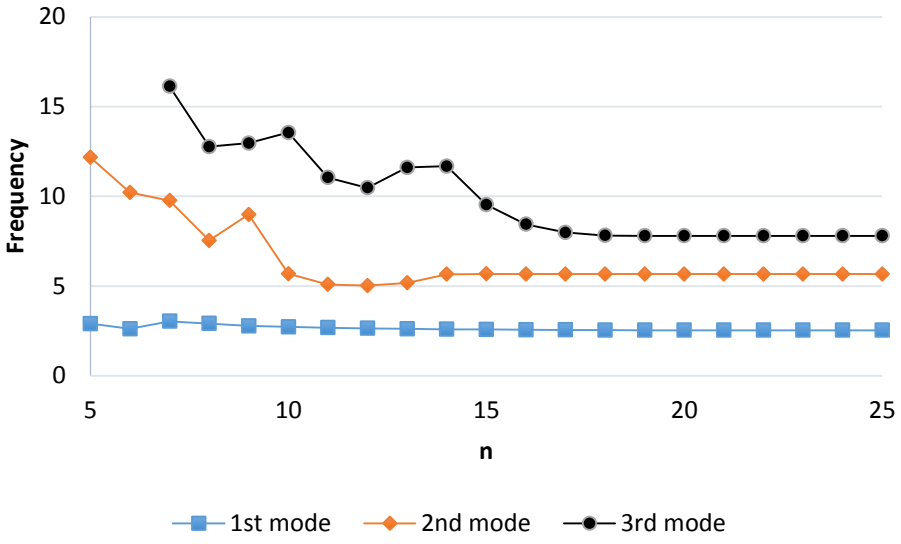

Figure 3.10 Convergence of natural frequencies for $K_0 = 1$ and $K_1 = 1$

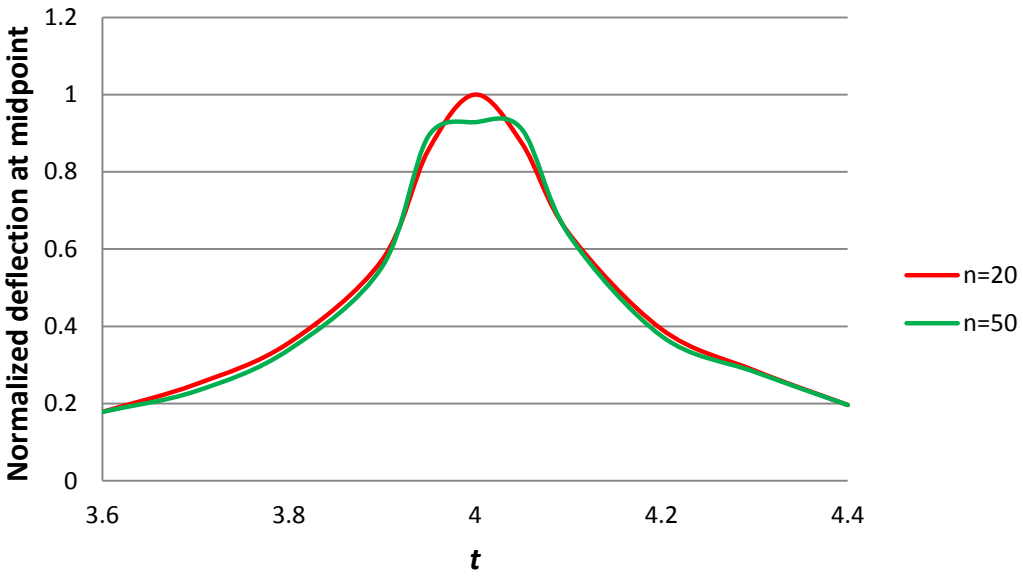

Figure 3.11 The effects on the vertical deflection of the beam's midpoint by a point force when $K_0 = 0$

The effect of a moving load at the middle of the beam was investigated. Firstly, the stiffness parameters were taken as $K_0 = 0$ and $K_1 = 0$, and the deflection at midpoint was calculated for time, t. Time is defined by $t = l/2v$, where l is the length of the beam, v is the velocity of the moving load. Figure 3.11 shows the deflection when $v = 50m/s$.

The effect of the shear parameter to the deflection at the middle of the beam was also analyzed. The result is presented in Figure 3.12 which shows that the shear parameter significantly affects the deflection of the beam under moving load. Increase in the shear parameter decreases the amplitude of deflection.

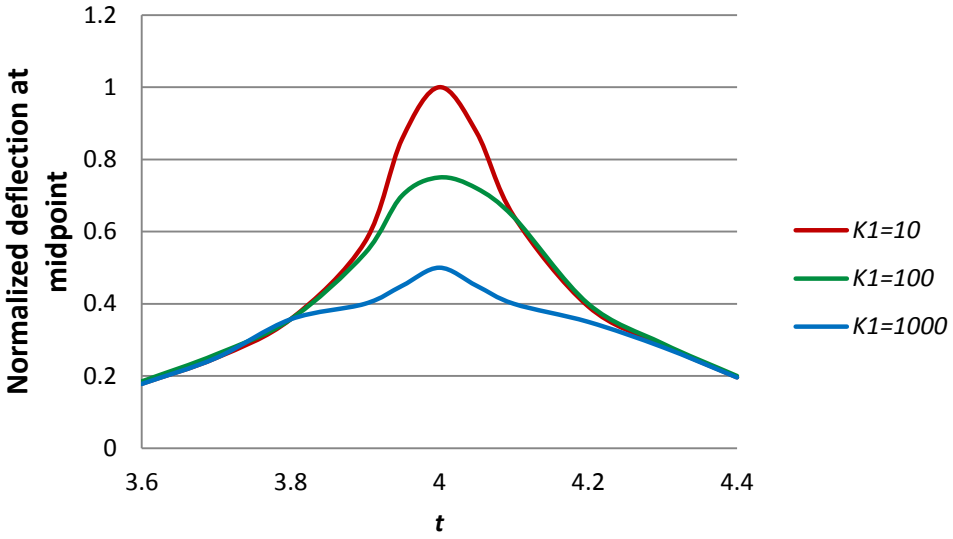

Figure 3.12 The effects on the vertical deflection of the beam's midpoint by a point force for different K_1

Chapter 4 – Extension of AMDM application to Special Case

4.1 Application of AMDM to a Euler-Bernoulli Beam with Axial Loading

The presence of an axial loading for slender beam makes it behave in a different way therefore needs to be considered. In the case of railway track which acts as a uniform slender beam axial loading can be caused by ambient temperature change which makes the beam expand and contract creating compressive forces. This condition is common in Kazakhstan due to the high variation of temperature.

Axially loaded Euler Bernoulli beam resting on one parameter Winkler foundation, as shown in Figure 4.1, is investigated, and natural vibrations are calculated using Adomian Modified Decomposition Method which is described in Chapter 2. The effect of axial loading for natural frequency is investigated by increasing it and applying for different boundary conditions.

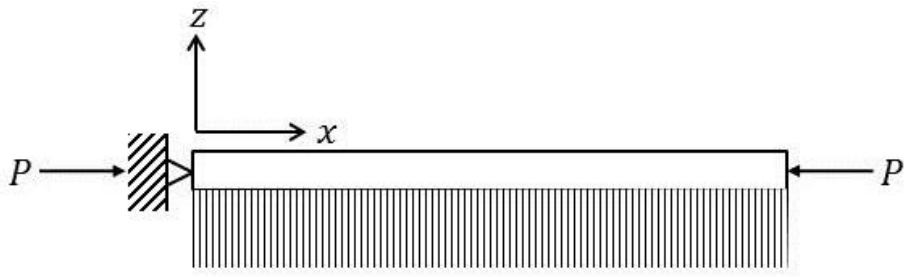

Figure 4.1 Beam under axial loading while resting on an elastic foundation

Governing equation is obtained by adding axial loading term for Eq. (2.4) from Chapter 2. The external work done by the axial load is

$$W = \frac{P}{2}\int_0^l \left(\frac{\partial w(x,t)}{\partial x}\right)^2 \mathrm{d}x. \tag{4.1}$$

By using Hamilton's principle and using the Lagrangian of the system

$$\delta \int_{t_1}^{t_2} (T - U + W)\mathrm{d}t = 0. \tag{4.2}$$

Eq. (2.4) now can be extended to

$$EI\frac{\partial^4 w(x,t)}{\partial x^4} + \rho A\frac{\partial^2 w(x,t)}{\partial t^2} + P\frac{\partial^2 w(x,t)}{\partial x^2} + k_w w(x,t) - \frac{EA}{2l}\frac{\partial^2 w(x,t)}{\partial x^2}\int_0^l \left(\frac{\partial w(x,t)}{\partial x}\right)^2 \mathrm{d}x = 0. \tag{4.3}$$

After separating $w(x,t)$ in space and time according to modal analysis of harmonic free vibration, Eq. (4.3) reduces to

$$EI\frac{\mathrm{d}^4\phi(x)}{\mathrm{d}x^4} + P\frac{\mathrm{d}^2\phi(x)}{\mathrm{d}x^2} - \frac{EA}{2l}\frac{\mathrm{d}^2\phi(x)}{\mathrm{d}x^2}\int_0^l \left(\frac{\mathrm{d}\phi(x)}{\mathrm{d}x}\right)^2 \mathrm{d}x + k_w\phi(x) - \rho A\omega^2\phi(x) = 0. \tag{4.4}$$

Eq. (4.4) is now made non-dimensional using

$$X = \frac{x}{l},\ \ \phi(X) = \frac{\phi(x)}{l}, \qquad \bar{P} = \frac{Pl^2}{EI},\ \ K_0 = \frac{k_w l^4}{EI},\ \ \lambda = \frac{\rho A\omega^2 l^4}{EI},$$

and becomes

$$\frac{\mathrm{d}^4\phi(X)}{\mathrm{d}X^4} + \bar{P}\frac{\mathrm{d}^2\phi(X)}{\mathrm{d}X^2} - \frac{1}{2}\frac{\mathrm{d}^2\phi(X)}{\mathrm{d}X^2}\int_0^1 \left(\frac{\mathrm{d}\phi(X)}{\mathrm{d}X}\right)^2 \mathrm{d}X + (K_0 g(X) - \lambda)\phi(X) = 0. \tag{4.5}$$

4.1.1 Boundary conditions

For the analysis of axially loaded beam two boundary conditions are chosen, namely, clamped-clamped and clamped-free.

The boundary conditions for the clamped-clamped case at $X = 0$ and $X = 1$ are

$$\phi(X) = \frac{\mathrm{d}\phi(X)}{\mathrm{d}X} = 0. \tag{4.6}$$

The boundary conditions for the clamped-free case at $X = 0$ and $X = 1$ are

$$\phi(0) = \frac{\mathrm{d}\phi(0)}{\mathrm{d}X} = 0, \qquad \phi(1) = \frac{\mathrm{d}^3\phi(1)}{\mathrm{d}X} + \bar{P}\frac{\mathrm{d}\phi(X)}{\mathrm{d}X} \tag{4.7}$$

Boundary conditions described in terms of rotational and translational flexible ends from Figure 2.2 are as follows

$$\frac{\mathrm{d}^2\phi(0)}{\mathrm{d}X^2} - \kappa_{L0}\frac{\mathrm{d}\phi(0)}{\mathrm{d}X} = 0$$

$$\frac{\mathrm{d}^3\phi(0)}{\mathrm{d}X^3} + \kappa_{L1}\phi(0) = 0$$

$$\frac{\mathrm{d}^2\phi(1)}{\mathrm{d}X^2} + \kappa_{R0}\frac{\mathrm{d}\phi(1)}{\mathrm{d}X} = 0 \tag{4.8}$$

$$\frac{\mathrm{d}^3\phi(1)}{\mathrm{d}X^3} + \bar{P}\frac{\mathrm{d}\phi(1)}{\mathrm{d}X} - \kappa_{R1}\phi(1) = 0$$

4.1.2 Application of the Adomian Modified Decomposition Method

AMDM is applied using the same method as described in Chapter 3.1. Firstly, Eq. (4.5) is integrated using four fold operator $G^{-1} = \int_0^x \int_0^x \int_0^x \int_0^x (\cdots)\mathrm{d}X\mathrm{d}X\mathrm{d}X\mathrm{d}X$ as

$$\phi(X) = \Phi(X) - G^{-1}\left\{\bar{P}\frac{\mathrm{d}^2\phi(X)}{\mathrm{d}X^2} - \frac{1}{2}\frac{\mathrm{d}^2\phi(X)}{\mathrm{d}X^2}\int_0^1\left(\frac{\mathrm{d}\phi(X)}{\mathrm{d}X}\right)^2\mathrm{d}X + (K_0 - \lambda)\phi(X)\right\}. \tag{4.9}$$

By substituting Eq. (3.14) for the nonlinear term, and using $\phi(\mathrm{X}) = \sum_{\mathrm{m}=0}^{\infty}\mathrm{C_m X^m}$ and its derivatives Eq. (4.9) now becomes

$$\phi(X) = \Phi(X) + G^{-1}\left\{-\bar{P}\sum_{m=0}^{\infty}(m+1)(m+2)C_{m+2}X^m + \sum_{m=0}^{\infty}\zeta_m X^m - (K_0 - \lambda)\sum_{m=0}^{\infty}C_m X^m\right\} \tag{4.10}$$

The first 4 terms of coefficients C_m are as in Eq. (3.17) and C_m for $m \geq 4$ as following

$$C_m = \frac{1}{m(m-1)(m-2)(m-3)}\sum_{j=0}^{m-4}\left[-\bar{P}(j+1)(j+2)C_{j+2} + \zeta_j\right. \tag{4.11}$$

$$-(K_0 - \lambda)C_j \,]$$

4.1.3 Results

Clamped-Free Uniform Beam

The first case analyzed is the clamped-free uniform beam resting on an the Winkler foundation and experiencing axial compressive force.

The boundary conditions are as given in Eqs. (4.7) and (4.8) with the spring constants leading to, $\kappa_{L0} \to \infty, \kappa_{R0} \to 0, \kappa_{L1} = \infty, \kappa_{R1} = 0$. From Eq. (3.20) and Eq. (4.8) with $X = 0$ and $X = 1$ following algebraic equations can be formulated

$$\sum_{m=0}^{n-3}(m+1)(m+2)C_{m+2} + \kappa_{R0}\sum_{m=0}^{n-2}(m+1)C_{m+1} =$$

$$f_{11}^{[n]}(\lambda)C_0 + f_{12}^{[n\}}(\lambda)C_1 = 0$$

$$\sum_{m=0}^{n-4}(m+1)(m+2)(m+3)C_{m+3} + \bar{P}\sum_{m=0}^{n-2}(m+1)C_{m+1} \tag{4.12}$$

$$-\kappa_{R1}\sum_{m=0}^{n-1}C_m = f_{21}^{[n]}(\lambda)C_0 + f_{22}^{[n]}(\lambda)C_1 = 0$$

Firstly calculations were made for clamped-free beam resting on an elastic foundation for $\bar{P} = 0$, and $K_0 = 1$ with, and without, the non-linear term in Eq. (4.10). Results are obtained for the first 4 modes and compared with results from literature [30] as shown in Table 4.1. Here $\Omega_{non(i)}$ stands for natural frequency

with non-linear term, and $\Omega_{n(i)}$ is natural frequency without using the non-linear term.

Table 4.1 Natural frequencies of clamped free beam on an elastic foundation with $\bar{P} = 0$, and $K_0 = 1$

Mode (i)	Ref. [30] $\Omega_{n(i)}$	Present $\Omega_{n(i)}$	Present $\Omega_{non(i)}$	Present $\Omega_{non(i)} / \Omega_{n(i)}$
1	3.66	3.6712	3.9869	1.089
2	22.22	22.2343	24.4049	1.098
3	62.69	62.7421	69.1014	1.101
4	124.29	124.3811	138.0632	1.111

Table 4.1 shows that the results are just slightly higher than the results of Ref. [30]. Table 4.1 also shows the results of natural frequencies with the non-linear term, and the ratio of results with and without non-linear term is provided. It can be seen that natural frequencies are higher with the presence of the non-linear term and its affect increases as with the increase of modes.

Figure 4.2 shows the effect of axial force and foundation stiffness for natural frequency modes. When varying the axial force, the elastic stiffness was held constant, and vice-versa. In can be seen that the first mode is mostly affected by both axial force and stiffness increase than higher modes. Axial force affects other modes significantly as well, compared to the stiffness parameter.

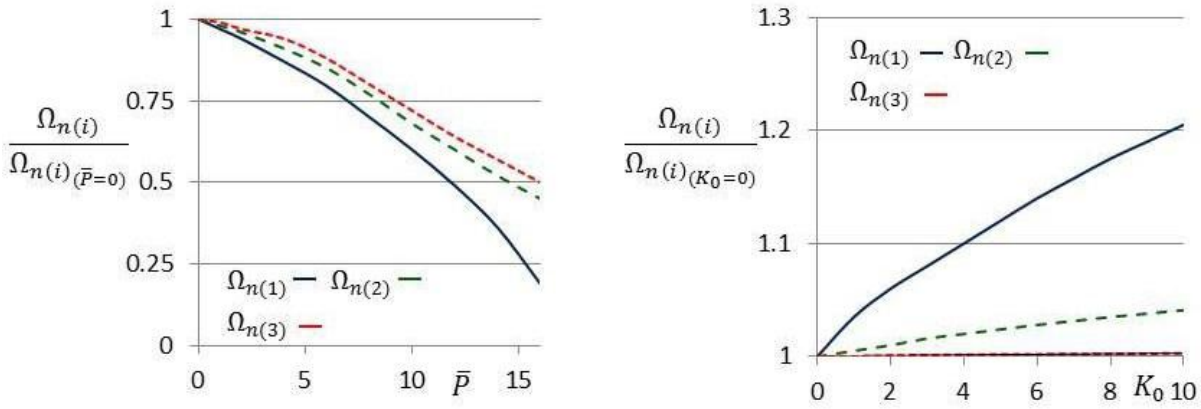

Figure 4.2 Effect of the axial force and foundation stiffness for frequency modes

By substituting obtained $\Omega_{n(1)}$ back into Eqs. (4.11) and (3.23) and normalizing it using Eq. (3.24), a polynomial is derived that describes the first mode shape function. Other natural frequencies modes shapes are obtained in the same way. Figure 4.3 illustrates the first and the third mode shape functions of natural frequencies and the effect of different values of axial force. It can be seen that axial force does not affect the mode shape much. As expected the negative axial force creates tension in the beam and decreases the transverse deflection while positive axial force creates compression and induces the vibration for the first mode, however has less effect on the third mode. The stiffness parameter was kept constant while changing the axial force.

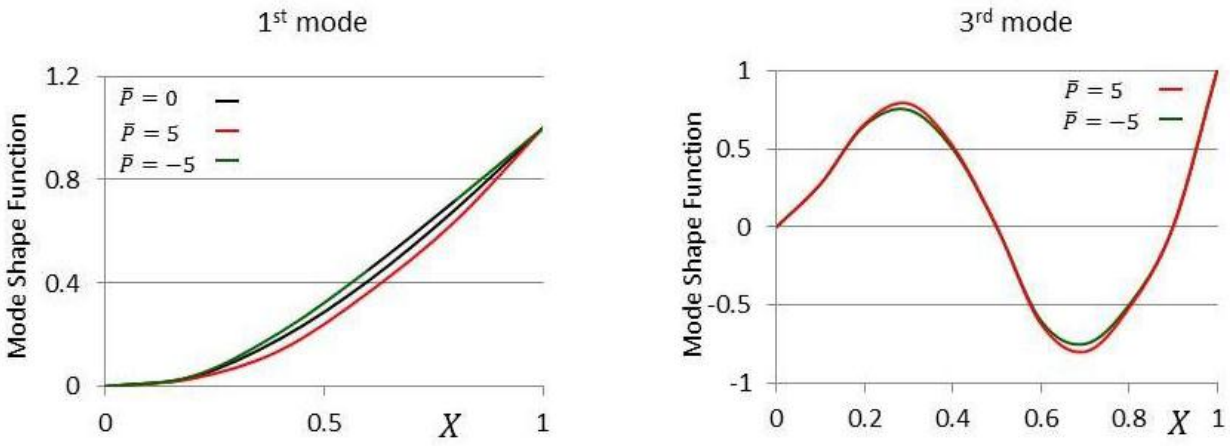

Figure 4.3 First and third mode shapes for various axial loads with $K_0 = 1$

The speed of the convergence and obtaining accurate results were the main objectives of this study. The AMDM method provided fast convergence especially with results for the first mode as shown in Figure 4.5.

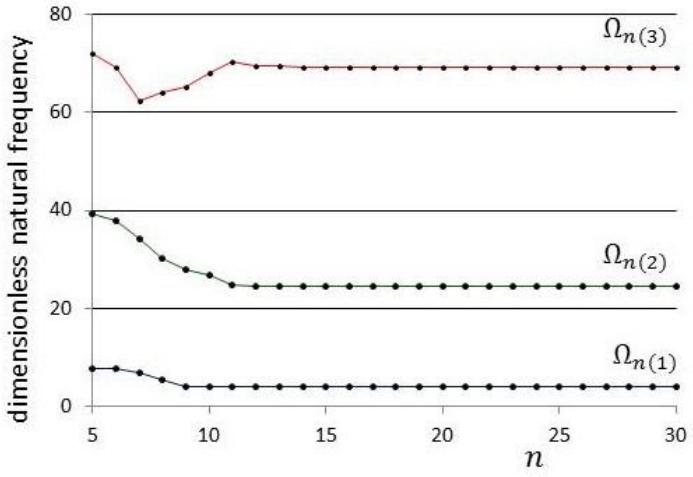

Figure 4.4 Convergence of natural frequencies for $\overline{P} = 0$ and $K_0 = 1$

Clamped-Clamped Uniform Beam

The boundary conditions for clamped-clamped beam are as given in Eqs. (4.6) and (4.8) with the spring constants becoming, $\kappa_{L0} \to \infty, \kappa_{R0} \to 0, \kappa_{L1} =$

$\infty, \kappa_{R1} = 0$. From Eq. (3.20) and Eq. (4.8) with $X = 0$ and $X = 1$ following algebraic equations can be formulated

$$\sum_{m=0}^{n-1} C_m = f_{11}^{[n]}(\lambda)C_0 + f_{12}^{[n]}(\lambda)C_1 = 0$$

$$\sum_{m=0}^{n-2} (m+1)C_{m+1} = f_{21}^{[n]}(\lambda)C_0 + f_{22}^{[n]}(\lambda)C_1 = 0$$

Natural frequencies of clamped-clamped beam were calculated for two different foundation stiffness values while keeping axial force zero, and compared with other results from literature. Table 4.3 shows that the results from current method agree with those reported in the literature.

Table 4.2 Natural frequencies of clamped-clamped beam on an elastic foundation with $\bar{P} = 0$ and without the non-linear term

	$K_0 = 0$			$K_0 = 100$		
	Present	Ref.[31]	Ref[32]	Present	Ref. [31]	Ref. [32]
$\Omega_{n(1)}$	4.73004	4.7314	4.73	4.95246	4.9515	4.95
$\Omega_{n(2)}$	7.85320	7.8533	7.854	7.91103	7.9044	7.904
$\Omega_{n(3)}$	10.9955	10.9908	10.996	11.0121	11.0096	11.014

In Table 4.3 results for the first four modes with and without the non-linear term are shown. Present results are quite the same as in Ref. [34]. However, natural frequencies with the non-linear term again become higher.

And from the ratios presented in Table 4.3 it can be seen that it has greater affect for higher modes.

Table 4.3 Natural frequencies of clamped-clamped beam on an elastic foundation with $\overline{P} = 0$, and $K_0 = 1$

Mode (i)	Ref. [33] $\Omega_{n(i)}$	Present $\Omega_{n(i)}$	Present $\Omega_{non(i)}$	Present $\Omega_{non(i)} / \Omega_{n(i)}$
1	22.435	22.614	23.971	1.06
2	62.094	62.051	74.461	1.19
3	122.659	123.54	149.772	1.21
4	204.935	205.332	256.665	1.25

Calculated natural frequencies are used to develop a polynomial for the first three mode shape functions using Eqs. (4.11), (3.23) and (3.24). Normalised mode shapes of the first three modes are shown in Figure (4.5).

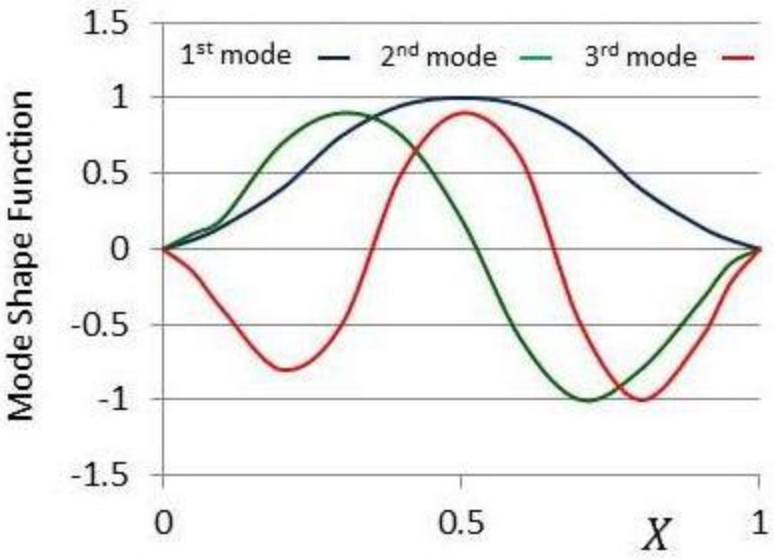

Figure 4.5 Normalized mode shapes for the first three modes for a clamped-clamped beam with $\overline{P} = 1$ and $K_0 = 1$

Chapter 5 – Concluding Remarks

Analytical solution technique, namely Adomian Modified Decomposition method was developed that provides fast, efficient and accurate results for the fourth-order nonlinear differential equations describing the transverse vibrations of a beam on an elastic foundation. AMDM has advantages of solving without discretization, linearization, perturbation, or a priori assumptions, all of which has the potential to change the physics of the problem. The accuracy of the method was validated. Fast and accurate convergences of results, especially for the first vibration mode, were observed and presented in all applications of AMDM considered in the present work. Solution algorithm based on the AMDM was developed to determine the vibration frequency of a beam which is relatively easy to apply boundary conditions. Corresponding parameters can simply be changed for new results without repeating the solution algorithms. Beams were mostly analyzed using Euler-Bernoulli beam theory. However, it should be noted that despite the effectiveness of the Euler-Bernoulli beam theory on analyzing vibration frequencies of slender beams, the Timoshenko beam theory predicts more accurate results on thick non-slender beams where shear or rotatory effects needs to be considered. It was found that the presence of non-linear term in the governing equation increases the beam vibration frequency. Also frequency increases along with the increase of both stiffness and shear parameter of the foundation. However, change is noticeable only at

greater values of coefficients. After the analysis of beam resting on two-parameter Pasternak foundation, it was found that shear parameter of the foundation had greater effect on the frequency than stiffness parameter. Moreover, investigation of beam subjected to harmonic moving loading showed that the amplitude of beam deflection decreases as shear coefficient of foundation increases. Finally, beam resting on Winkler foundation and subjected to axial force was analyzed. Results show that axial force mostly affects the first mode shape.

References

[1] A.M. Wazwaz. A reliable modification of Adomian's decomposition method. Appl. Math. Comput., 102 (1999), pp. 77-86

[2] A.M. Wazwaz., S.M. El-Sayed. A new modification of the Adomian decomposition method for linear and nonlinear operators. Appl. Math. Comput., 122: 3 (2001), pp. 393-405

[3] M. A. De Rosa, M. J. Maurizi. The influence of concentrated masses and Pasternak soil on the free vibrations of Euler beams - exact solution. J. Sound and Vibration, 212 (1998), pp. 573-581

[4] S. C. Dutta, R. Roy. A critical review on idealization and modeling for interaction among soil–foundation–structure system. Computers and Structures 80 (2002) pp.1579–1594

[5] M.H. Kargarnovin, D. Younesian. Dynamics of Timoshenko beams on Pasternak foundation under moving load. Mechanics Research Communications 31 (2004) pp. 713–723

[6] MM. Filonenko-Borodich. Some approximate theories of elastic foundation. Uchenyie Zapiski Moskovskogo Gosudarstvennogo Universiteta [in Russian] Mekhanica 46:3–18, (1940)

[7] Kerr AD. A study of a new foundation model. Act. Mech. I/2:135–47(1965).

[8] Vlasov VZ, Leontiev NN. Beams, plates and shells on an elastic foundation [in Russian] Moscow, USSR: Fizmatgiz; (1960).

[9] H. P. Lee. Dynamic response of a Timoshenko beam on a Winkler foundation subjected to a moving mass. Applied Acoustics, 55 (3) (1998) pp.203-215.

[10] D. Thambiratnam and Y. Zhuge. Dynamic analysis of beams on an elastic foundation subjected to moving loads. Journal of Sound and Vibration, 198 (1996) pp149-169.

[11] S. Kim. Vibration and Stability of axial loaded beams on elastic foundation under moving harmonic loads. Engineering Structures 26 (2004), pp. 95-105.

[12] M. H. Kargarnovin and D. Younesian, Response of beams on nonlinear viscoelastic foundations to harmonic moving loads, Computers & Structures, 83 (2005) 1865-1877.

[13] A.D Senalp, A. Arikoglu, I. Ozkol, V. Dogan. Dynamic response of a finite length Euler-Bernoulli beam on linear and nonlinear viscoelastic foundations to a concentrated moving force. Journal of Mechanical Science and Technology 24:10 (2010) pp. 1957~1961

[14] M. Balkaya, M. O. Kaya, and A. Saglamer. Analysis of the vibration of an elastic beam supported on elastic soil using the differential transform method. Archive of Applied Mechanics, 79: 2(2009) pp. 135–146.

[15] B. Ozturk and S. B. Coskun. The Homotopy Perturbation Method for free vibration analysis of beam on elastic foundation, Structural Engineering and Mechanics. 37: 4 (2011) pp. 415–425.

[16] C. N. Chen. Vibration of prismatic beam on an elastic foundation by the differential quadrature element method. Computers and Structures, 77:1(2000) pp. 1–9.

[17] J. H. He. Coupling method of a homotopy technique and a perturbation technique for non-linear problems. International Journal of Non-Linear Mechanics 35:1(2000) pp. 37–43.

[18] G. Adomian. Solving Frontier Problems of Physics. The Decomposition Method. Kluwer Academic Publishers, Boston, Mass., USA (1994).

[19] S. Coşkun, B. Öztürk, M. Mutman. Adomian Decomposition Method for vibration of nonuniform Euler Beams on elastic foundation. Department of Civil Engineering, Kocaeli University, Turkey (2014).

[20] D. Adair, M. Jaeger. Simulation of tapered rotating beams with centrifugal stiffening using the Adomian decomposition method. Applied Mathematical Modelling, 40 (2016) pp. 3230-3241
[21] Q. Mao. Application of Adomain modified method for free vibration analysis of rotating beams. Mathematical Problems in Engineering, Article ID 284720, 10 pages (2013).
[22] S. Das. A numerical solution of the vibration equation using modified decomposition method. J. Sound and Vibration, 320:3 (2009), pp. 576-583
[23] K. Abbaoni, and Y. Cherruault. Convergence of Adomian method applied to differential equations. Comp. Math. Appl., 103:9 (1994a)
[24] D. Lesnik. The Decomposition method for forward and backward time-dependent problems. Journal of Comp. and Appl. Math., 27:39 (2002)
[25] A. Wazwaz and S. Khuri. The decomposition method for solving a second kind Fredholm equation with a logarithmic kernel. J. Computer Math., 103:10 (1996)
[26] A. Wazwaz. A comparison between Adomian decomposition method and Taylor series method in the series solutions. Appl., Math. Comput., (1998) pp. 37-44
[27] T. Yokoyama. Vibrations of Timoshenko beam-columns on two-parameter elastic foundations. Earthquake Engineering & Structural Dynamics, 20:4 (1991) pp. 355 - 370
[28] A. S. da Costa Azevêdo, A. C. Vasconcelos, S. dos Santos Hoefel. Dynamic analysis of elastically supported Timoshenko beam. Revista Interdisciplinar de Pesquisa em Engenharia-RIPE, 2:34 (2016) pp.71-85
[29] MH Taha. General analysis of stressed beams on elastic foundation subjected to discontinuous loads. Ships and Offshore Structures, 12:3, (2017) pp.388-394
[30] G. Wang, N. M. Wereley. Free vibration analysis of rotating blades with uniform taper, AIAA J., 42, (2004) pp. 2429-2437
[31] W. Q. Chen, C. F. Lü, Z. G. Bian. A mixed method for bending and free vibration of beams resting on a Pasternak elastic foundation. Applied Mathematical Modelling, 28, (2004) pp. 877-890.
[32] M. A. De Rosa, M. J. Maurizi. The influence of concentrated masses and Pasternak soil on the free vibrations of Euler beams - exact solution. J. Sound and Vibration 212, (1998) pp.573-581
[33] C.-N Chen: Vibration of prismatic beam on an elastic foundation by the differential quadrature element method. Computers & Structures, 77, 1:9 (2000).

Appendices

Appendix A – MATLAB codes

A1. MATLAB code for Adomian polynomials

```
syms n L u(n) %L stands for lambda
nth=input('Enter n: ');
for N=0:nth
F=sin(symsum(L^n*u(n),n,0,N)); %example for sine. Function
creates series and summates
% What is in the brackets (symsum(L^n*u(n),n,0,N)) is the
function for any
% expession, just need to change what is outside as in
following forms:
%    sin(..)+cos(..)^2*sinh(..) etc. for trigonometric
%    (..)^4 for u^4 etc
%    log(..) for natural log, exp(..) for exponential
A=subs(diff(F,L,N),L,0)/factorial(N); %Differentiate F, then
substitute L by 0 then divide by n!
fprintf('\nA(%d)= %s\n',N,A) %
end
```

A2. MATLAB code for linear BVP

```
%Validation of ADM. Finding the error for linear BVP
clear
syms x
    A=[0.9740953834 0.99447891278 0.9989095252];
    B=[3.1897820557 3.0382130987 3.0073098797];
for n=1:3
    f0(n)=1+A(n)*x+x.^2+1/6*B(n)*x.^3+1/8*x.^4+1/24*x.^5;
    f1(n)=1/24*x.^4+(A(n)-1)/120*x.^5+(2-A(n))/720*x.^6+(B(n)-
2)/5040*x.^7+(3-B(n))/40320*x.^8+1/181440*x.^9;
end
    p1=(f0(1)+1/360*x.^6)+(f1(1)-1/1209600*x.^10-
1/19958400*x.^11);
    p2=(f0(2)+1/144*x.^6+1/1680*x.^7)+(f1(2)-1/19958400*x.^11-
1/159667200*x.^12);

p3=(f0(3)+1/144*x.^6+1/840*x.^7+1/10080*x.^8)+(f1(3)+1/3991680
0*x.^11-1/239500800*x.^12-1/1556755200*x.^13);
x=0:0.05:1;
    E1=1+x.*exp(x)-subs(p1);
    E2=1+x.*exp(x)-subs(p2);
    E3=1+x.*exp(x)-subs(p3);
plot(x,E1,'r',x,E2,'b',x,E3,'k')
xlabel('x')
```

```
ylabel('Error')
title('Error of ADM approximaiton compared to actual value for
linear BVP')
legend('E1','E2','E3')
```

A3. MATLAB code for nonlinear BVP

```
clear
syms x
    A=[0.9969706142 1.0006029353 0.9998909027];
    B=[1.0205416499 0.9960391622 1.0007021518];
for n=1:3
    y0(n)=1+A(n)*x+1/2*x.^2+B(n)/6*x.^3+1/24*x.^4;

A0(n)=1+2*A(n)*x+(1+A(n)^2)*x.^2+(B(n)/3+A(n))*x.^3+(1/3+A(n)*
B(n)/3)*x.^4+(A(n)/12+B(n)/6)*x.^5+(1/24+B(n)^2/36)*x.^6+B(n)/
72*x.^7+1/576*x.^8;
end

p1=y0(1)+int(int(int(int(int(A0(1),x,0,x)))))+int(int(int(int(
int(-x*A0(1),x,0,x)))));

p2=y0(2)+int(int(int(int(int(A0(2),x,0,x)))))+int(int(int(int(
int(-
x*A0(2),x,0,x)))))+int(int(int(int(int(x.^2/2*A0(2),x,0,x)))))
;

p3=y0(3)+int(int(int(int(int(A0(3),x,0,x)))))+int(int(int(int(
int(-
x*A0(3),x,0,x)))))+int(int(int(int(int(x.^2/2*A0(3),x,0,x)))))
+int(int(int(int(int(-x.^3/6*A0(3),x,0,x)))));
x=0:0.05:1;
    E1=abs(exp(x)-subs(p1));
    E2=abs(exp(x)-subs(p2));
    E3=abs(exp(x)-subs(p3));
plot(x,E1,'r',x,E2,'b',x,E3,'k')
xlabel('x')
ylabel('Error')
title('Error of ADM approximaiton compared to actual value for
NonLinear BVP')
legend('E1','E2','E3')
```

A4. MATLAB code for distributed harmonic loading function

```
s=2;
r=3;
V=10;
P0=10;% just example
L=input('Please enter L, number of separated impulses: ');
```

```
f=input('Please enter f, frequency of the moving load: ');
w=2*pi*f;
x=[-16:0.2:35];
t=0;
syms l
P = real(symsum(P0/2/r*cos(pi*(x-V*t-
(2*r+s)*l)./2/r).^2.*heaviside(r^2-(x-V*t-
(2*r+s)*l).^2).*exp(1i*w*t), l, 0, L-1));
plot(x,P*2*r/P0,'r')
a=sprintf('A series of distributed harmonic loads for s = %d
m, r = %d m, V = %d m/s, L = %d, f = %d',s,r,V,L,f);
title(a)
xlabel('x')
ylabel('P(x,t)[2r/P0]')
hold on
t=-1.1;
P = real(symsum(P0/2/r*cos(pi*(x-V*t-
(2*r+s)*l)./2/r).^2.*heaviside(r^2-(x-V*t-
(2*r+s)*l).^2).*exp(1i*w*t), l, 0, L-1));
plot(x,P*2*r/P0,'b--')
hold on
t=0.7;
P = real(symsum(P0/2/r*cos(pi*(x-V*t-
(2*r+s)*l)./2/r).^2.*heaviside(r^2-(x-V*t-
(2*r+s)*l).^2).*exp(1i*w*t), l, 0, L-1));
plot(x,P*2*r/P0,'k-.')
legend('when t=0','when t=-1.1','when t=0.7')
hold off
```

A5. MATLAB code for computing natural frequencies

```
clear all
syms C(m) C0 C1 K0 P L
nth=input('Enter n: ');
P=input('Enter P: ');
K0=input('Enter K0: ');
KL0=2;
KL1=6;
C2=KL0*C1/2;
C3=-KL1*C0/6;
i=1;
if i==1
    M=4;
    C4=subs(1/(M*(M-1)*(M-2)*(M-3))*symsum(-P*(m+1)*(m+2)*C(m+2)-(K0-L)*
      C(m)+(m+1)*C(m+1)*(M-m-3)*C(M-m-3)/2/(m+1)*(M-m-3)*(M-m-2)*C(M-m-2),
      m,0,M-4),[C(0),C(1),C(2)],[C0,C1,C2]);
    M=5;
    C5=subs(1/(M*(M-1)*(M-2)*(M-3))*symsum(-P*(m+1)*(m+2)*C(m+2)-(K0-L)*
      C(m)+(m+1)*C(m+1)*(M-m-3)*C(M-m-3)/2/(m+1)*(M-m-3)*(M-m-2)*C(M-m-
      2),m,0,M-4),[C(0),C(1),C(2), C(3)],[C0,C1,C2,C3]);
    M=6;
    C6=subs(1/(M*(M-1)*(M-2)*(M-3))*symsum(-P*(m+1)*(m+2)*C(m+2)-(K0-L)*
      C(m)+(m+1)*C(m+1)*(M-m-3)*C(M-m-3)/2/(m+1)*(M-m-3)*(M-m-2)*C(M-m-
      2),m,0,M-4),[C(0),C(1),C(2),C(3),C(4)],[C0,C1,C2,C3,C4]);
```

```
M=7;
C7=subs(1/(M*(M-1)*(M-2)*(M-3))*symsum(-P*(m+1)*(m+2)*C(m+2)-(K0-L)*
  C(m)+(m+1)*C(m+1)*(M-m-3)*C(M-m-3)/2/(m+1)*(M-m-3)*(M-m-2)*C(M-m-
  2),m,0,M-4),[C(0),C(1),C(2),C(3),C(4),C(5)],[C0,C1,C2,C3,C4,C5]);
M=8;
C8=subs(1/(M*(M-1)*(M-2)*(M-3))*symsum(-P*(m+1)*(m+2)*C(m+2)-(K0-L)*
  C(m)+(m+1)*C(m+1)*(M-m-3)*C(M-m-3)/2/(m+1)*(M-m-3)*(M-m-2)*C(M-m-
  2),m,0,M-
  4),[C(0),C(1),C(2),C(3),C(4),C(5),C(6)],[C0,C1,C2,C3,C4,C5,C6]);
M=9;
C9=subs(1/(M*(M-1)*(M-2)*(M-3))*symsum(-P*(m+1)*(m+2)*C(m+2)-(K0-L)*
  C(m)+(m+1)*C(m+1)*(M-m-3)*C(M-m-3)/2/(m+1)*(M-m-3)*(M-m-2)*C(M-m-
  2),m,0,M-
  4),[C(0),C(1),C(2),C(3),C(4),C(5),C(6),C(7)],[C0,C1,C2,C3,C4,C5,C6,C7
  ]);
M=10;
C10=subs(1/(M*(M-1)*(M-2)*(M-3))*symsum(-P*(m+1)*(m+2)*C(m+2)-(K0-L)*
  C(m)+(m+1)*C(m+1)*(M-m-3)*C(M-m-3)/2/(m+1)*(M-m-3)*(M-m-2)*C(M-m-
  2),m,0,M-
  4),[C(0),C(1),C(2),C(3),C(4),C(5),C(6),C(7),C(8)],[C0,C1,C2,C3,C4,C5,
  C6,C7,C8]);
M=11;
C11=subs(1/(M*(M-1)*(M-2)*(M-3))*symsum(-P*(m+1)*(m+2)*C(m+2)-(K0-L)*
  C(m)+(m+1)*C(m+1)*(M-m-3)*C(M-m-3)/2/(m+1)*(M-m-3)*(M-m-2)*C(M-m-
  2),m,0,M-
  4),[C(0),C(1),C(2),C(3),C(4),C(5),C(6),C(7),C(8),C(9)],[C0,C1,C2,C3,C
  4,C5,C6,C7,C8,C9]);
M=12;
C12=subs(1/(M*(M-1)*(M-2)*(M-3))*symsum(-P*(m+1)*(m+2)*C(m+2)-(K0-L)*
  C(m)+(m+1)*C(m+1)*(M-m-3)*C(M-m-3)/2/(m+1)*(M-m-3)*(M-m-2)*C(M-m-2),
  m,0,M-4),[C(0),C(1),C(2),C(3),C(4),C(5),C(6),C(7),C(8),C(9),C(10)],
  [C0,C1,C2,C3,C4,C5,C6,C7,C8,C9,C10]);
M=13;
C13=subs(1/(M*(M-1)*(M-2)*(M-3))*symsum(-P*(m+1)*(m+2)*C(m+2)-(K0-L)*
  C(m)+(m+1)*C(m+1)*(M-m-3)*C(M-m-3)/2/(m+1)*(M-m-3)*(M-m-2)*C(M-m-
  2),m,0,M-4),[C(0),C(1),C(2),C(3),C(4),C(5),C(6),C(7),C(8),C(9),
  C(10),C(11)],[C0,C1,C2,C3,C4,C5,C6,C7,C8,C9,C10,C11]);
M=14;
C14=subs(1/(M*(M-1)*(M-2)*(M-3))*symsum(-P*(m+1)*(m+2)*C(m+2)-(K0-L)*
  C(m)+(m+1)*C(m+1)*(M-m-3)*C(M-m-3)/2/(m+1)*(M-m-3)*(M-m-2)*C(M-m-
  2),m,0,M-
  4),[C(0),C(1),C(2),C(3),C(4),C(5),C(6),C(7),C(8),C(9),C(10),C(11),C(1
  2)], [C0,C1,C2,C3,C4,C5,C6,C7,C8,C9,C10,C11,C12]);
M=15;
C15=subs(1/(M*(M-1)*(M-2)*(M-3))*symsum(-P*(m+1)*(m+2)*C(m+2)-(K0-L)*
  C(m)+(m+1)*C(m+1)*(M-m-3)*C(M-m-3)/2/(m+1)*(M-m-3)*(M-m-2)*C(M-m-
  2),m,0,M-
  4),[C(0),C(1),C(2),C(3),C(4),C(5),C(6),C(7),C(8),C(9),C(10),C(11),C(1
  2),C(13)],[C0,C1,C2,C3,C4,C5,C6,C7,C8,C9,C10,C11,C12,C13]);
M=16;
C16=subs(1/(M*(M-1)*(M-2)*(M-3))*symsum(-P*(m+1)*(m+2)*C(m+2)-(K0-L)*
  C(m)+(m+1)*C(m+1)*(M-m-3)*C(M-m-3)/2/(m+1)*(M-m-3)*(M-m-2)*C(M-m-
  2),m,0,M-
  4),[C(0),C(1),C(2),C(3),C(4),C(5),C(6),C(7),C(8),C(9),C(10),C(11),C(1
  2),C(13),C(14)],[C0,C1,C2,C3,C4,C5,C6,C7,C8,C9,C10,C11,C12,C13,C14]);
M=17;
C17=subs(1/(M*(M-1)*(M-2)*(M-3))*symsum(-P*(m+1)*(m+2)*C(m+2)-(K0-L)*
  C(m)+(m+1)*C(m+1)*(M-m-3)*C(M-m-3)/2/(m+1)*(M-m-3)*(M-m-2)*C(M-m-
  2),m,0,M-
  4),[C(0),C(1),C(2),C(3),C(4),C(5),C(6),C(7),C(8),C(9),C(10),C(11),C(1
```

```
      2),C(13),C(14),C(15)],[C0,C1,C2,C3,C4,C5,C6,C7,C8,C9,C10,C11,C12,C13,
      C14,C15]);
    M=18;
    C18=subs(1/(M*(M-1)*(M-2)*(M-3))*symsum(-P*(m+1)*(m+2)*C(m+2)-(K0-L)*
      C(m)+(m+1)*C(m+1)*(M-m-3)*C(M-m-3)/2/(m+1)*(M-m-3)*(M-m-2)*C(M-m-
      2),m,0,M-
      4),[C(0),C(1),C(2),C(3),C(4),C(5),C(6),C(7),C(8),C(9),C(10),C(11),C(1
      2),C(13),C(14),C(15),C(16)],[C0,C1,C2,C3,C4,C5,C6,C7,C8,C9,C10,C11,C1
      2,C13,C14,C15,C16]);
end
for n=4:nth
  F1=subs(symsum((m+1)*(m+2)*C(m+2),m,0,n-
    3),[C(0),C(1),C(2),C(3),C(4),C(5),
    C(6),C(7),C(8),C(9),C(10),C(11),C(12),C(13),C(14),C(15),C(16),C(17),C(
    18)],
    [C0,C1,C2,C3,C4,C5,C6,C7,C8,C9,C10,C11,C12,C13,C14,C15,C16,C17,C18]);
  F2=subs(symsum((m+1)*(m+2)*(m+3)*C(m+3),m,0,n-
    4)+P*symsum((m+1)*C(m+1),m,0, n-
    2),[C(0),C(1),C(2),C(3),C(4),C(5),C(6),C(7),C(8),C(9),C(10),C(11),C(12
    ),
    C(13),C(14),C(15),C(16),C(17),C(18)],[C0,C1,C2,C3,C4,C5,C6,C7,C8,C9,C1
    0, C11,C12,C13,C14,C15,C16,C17,C18]);
      f11=subs(F1,[C0,C1],[1,0]);
      f12=subs(F1,[C0,C1],[0,1]);
      f21=subs(F2,[C0,C1],[1,0]);
      f22=subs(F2,[C0,C1],[0,1]);
  p=f11*f22-f12*f21;
  fprintf('at n=%d (K0=%d, P=%d)',n,K0,P)
  format shortg
  lambda=flip(roots(sym2poly(p)))
end
```

A6. MATLAB code for computing mode shape functions

```
syms K0
for K0=[1]
    clear C0 C1 L X
    syms C(m) L X C1 C0
nth=input('Enter n: ');
KL0=1;
KL1=1;
g=1; % gamma
C2=KL0*C1/2;
C3=-KL1*C0/6;
i=1;
if i==1
    M=4;
    C4=subs(1/(M*(M-1)*(M-2)*(M-3))*symsum(-L/g*(m+1)*(m+2)*C(m+2)-(K0-
L)*C(m),m,0,M-4),[C(0),C(1),C(2)],[C0,C1,C2]);
    M=5;
    C5=subs(1/(M*(M-1)*(M-2)*(M-3))*symsum(-L/g*(m+1)*(m+2)*C(m+2)-(K0-
L)*C(m),m,0,M-4),[C(0),C(1),C(2), C(3)],[C0,C1,C2,C3]);
    M=6;
    C6=subs(1/(M*(M-1)*(M-2)*(M-3))*symsum(-L/g*(m+1)*(m+2)*C(m+2)-(K0-
L)*C(m),m,0,M-4),[C(0),C(1),C(2),C(3),C(4)],[C0,C1,C2,C3,C4]);
    M=7;
    C7=subs(1/(M*(M-1)*(M-2)*(M-3))*symsum(-L/g*(m+1)*(m+2)*C(m+2)-(K0-
L)*C(m),m,0,M-4),[C(0),C(1),C(2),C(3),C(4),C(5)],[C0,C1,C2,C3,C4,C5]);
```

```
    M=8;
    C8=subs(1/(M*(M-1)*(M-2)*(M-3))*symsum(-L/g*(m+1)*(m+2)*C(m+2)-(K0-
L)*C(m),m,0,M-
4),[C(0),C(1),C(2),C(3),C(4),C(5),C(6)],[C0,C1,C2,C3,C4,C5,C6]);
    M=9;
    C9=subs(1/(M*(M-1)*(M-2)*(M-3))*symsum(-L/g*(m+1)*(m+2)*C(m+2)-(K0-
L)*C(m),m,0,M-
4),[C(0),C(1),C(2),C(3),C(4),C(5),C(6),C(7)],[C0,C1,C2,C3,C4,C5,C6,C7]);
    M=10;
    C10=subs(1/(M*(M-1)*(M-2)*(M-3))*symsum(-L/g*(m+1)*(m+2)*C(m+2)-(K0-
L)*C(m),m,0,M-
4),[C(0),C(1),C(2),C(3),C(4),C(5),C(6),C(7),C(8)],[C0,C1,C2,C3,C4,C5,C6,C7,
C8]);
    M=11;
    C11=subs(1/(M*(M-1)*(M-2)*(M-3))*symsum(-L/g*(m+1)*(m+2)*C(m+2)-(K0-
L)*C(m),m,0,M-
4),[C(0),C(1),C(2),C(3),C(4),C(5),C(6),C(7),C(8),C(9)],[C0,C1,C2,C3,C4,C5,C
6,C7,C8,C9]);
    M=12;
    C12=subs(1/(M*(M-1)*(M-2)*(M-3))*symsum((-L/g)*(m+1)*(m+2)*C(m+2)-(K0-
L)*C(m),m,0,M-
4),[C(0),C(1),C(2),C(3),C(4),C(5),C(6),C(7),C(8),C(9),C(10)],[C0,C1,C2,C3,C
4,C5,C6,C7,C8,C9,C10]);
    M=13;
    C13=subs(1/(M*(M-1)*(M-2)*(M-3))*symsum((-L/g)*(m+1)*(m+2)*C(m+2)-(K0-
L)*C(m),m,0,M-
4),[C(0),C(1),C(2),C(3),C(4),C(5),C(6),C(7),C(8),C(9),C(10),C(11)],[C0,C1,C
2,C3,C4,C5,C6,C7,C8,C9,C10,C11]);
    M=14;
    C14=subs(1/(M*(M-1)*(M-2)*(M-3))*symsum((-L/g)*(m+1)*(m+2)*C(m+2)-(K0-
L)*C(m),m,0,M-
4),[C(0),C(1),C(2),C(3),C(4),C(5),C(6),C(7),C(8),C(9),C(10),C(11),C(12)],[C
0,C1,C2,C3,C4,C5,C6,C7,C8,C9,C10,C11,C12]);
    M=15;
    C15=subs(1/(M*(M-1)*(M-2)*(M-3))*symsum((-L/g)*(m+1)*(m+2)*C(m+2)-(K0-
L)*C(m),m,0,M-
4),[C(0),C(1),C(2),C(3),C(4),C(5),C(6),C(7),C(8),C(9),C(10),C(11),C(12),C(1
3)],[C0,C1,C2,C3,C4,C5,C6,C7,C8,C9,C10,C11,C12,C13]);
    M=16;
    C16=subs(1/(M*(M-1)*(M-2)*(M-3))*symsum((-L/g)*(m+1)*(m+2)*C(m+2)-(K0-
L)*C(m),m,0,M-
4),[C(0),C(1),C(2),C(3),C(4),C(5),C(6),C(7),C(8),C(9),C(10),C(11),C(12),C(1
3),C(14)],[C0,C1,C2,C3,C4,C5,C6,C7,C8,C9,C10,C11,C12,C13,C14]);
    M=17;
    C17=subs(1/(M*(M-1)*(M-2)*(M-3))*symsum((-L/g)*(m+1)*(m+2)*C(m+2)-(K0-
L)*C(m),m,0,M-
4),[C(0),C(1),C(2),C(3),C(4),C(5),C(6),C(7),C(8),C(9),C(10),C(11),C(12),C(1
3),C(14),C(15)],[C0,C1,C2,C3,C4,C5,C6,C7,C8,C9,C10,C11,C12,C13,C14,C15]);
    M=18;
    C18=subs(1/(M*(M-1)*(M-2)*(M-3))*symsum((-L/g)*(m+1)*(m+2)*C(m+2)-(K0-
L)*C(m),m,0,M-
4),[C(0),C(1),C(2),C(3),C(4),C(5),C(6),C(7),C(8),C(9),C(10),C(11),C(12),C(1
3),C(14),C(15),C(16)],[C0,C1,C2,C3,C4,C5,C6,C7,C8,C9,C10,C11,C12,C13,C14,C1
5,C16]);
end
for n=7:nth
F1=subs(symsum(C(m),m,0,n-
1),[C(0),C(1),C(2),C(3),C(4),C(5),C(6),C(7),C(8),C(9),C(10),C(11),C(12),C(1
3),C(14),C(15),C(16),C(17),C(18)],[C0,C1,C2,C3,C4,C5,C6,C7,C8,C9,C10,C11,C1
2,C13,C14,C15,C16,C17,C18]);
```

```
F2=subs(symsum((m+1)*C(m+1),m,0,n-
2),[C(0),C(1),C(2),C(3),C(4),C(5),C(6),C(7),C(8),C(9),C(10),C(11),C(12),C(1
3),C(14),C(15),C(16),C(17),C(18)],[C0,C1,C2,C3,C4,C5,C6,C7,C8,C9,C10,C11,C1
2,C13,C14,C15,C16,C17,C18]);
    f11=subs(F1,[C0,C1],[1,0]);
    f12=subs(F1,[C0,C1],[0,1]);
    f21=subs(F2,[C0,C1],[1,0]);
    f22=subs(F2,[C0,C1],[0,1]);
p=f11*f22-f12*f21;
%fprintf('at n=%d (K0=%d, K1=%d)',n,K0,K1)
format shortg
lambda=flip(roots(sym2poly(p)))
L=real(lambda(3));
omega=L^0.5;
disp(omega)
end
C0=0.1;
f21=eval(f21);
f22=eval(f22);
C1=-f21/f22*C0;
C2=eval(C2);
C3=eval(C3);
C4=eval(C4);
C5=eval(C5);
C6=eval(C6);
C7=eval(C7);
C8=eval(C8);
C9=eval(C9);
C10=eval(C10);
C11=eval(C11);
C12=eval(C12);
C13=eval(C13);
C14=eval(C14);
C15=eval(C15);
C16=eval(C16);
C17=eval(C17);
C18=eval(C18);
ph=0+C1*X^1+C2*X^2+C3*X^3+C4*X^4+C5*X^5+C6*X^6+C7*X^7+C8*X^8+C9*X^9+C10*X^1
0+C11*X^11+C12*X^12+C13*X^13+C14*X^14+C15*X^15+C16*X^16+C17*X^17+C18*X^18;
ph=ph/(int((ph)^2,X,0,1))^0.5;
X=0:0.05:1;
ph=eval(ph);
plot(X,ph,'r')
xlabel('X')
ylabel('phi-normolised')
hold on
end
```